

EMANUEL BOMBASARO

TITAN 1



FLIGHT DATA REPORT

Copyright © 2016 Emanuel Bombasaro

contact via e-mail at titan.hab@gmail.com.

This document is distributed in the hope that it will be useful, but without any warranty, without even the implied warranty of merchantability or fitness for a particular purpose. No guarantee is given for the accuracy, precision or reliability of the calculations, code and data stated, and you use it entirely at your own risk.

Permission is granted to distribute verbatim copies of this document and included source code. You are allowed to modify one or all of the source code files if and only if you change the name of the modified file. You are allowed to distribute the modified files but only together with the unmodified versions. You have to document all changes and the name of the author of the changes. No other permissions to copy or distribute this file in any form are granted. You are not allowed to take money for the distribution or use of either this file or a changed version, except for a nominal charge for copying etc..

Update published, April 2016

Titan

1. Greek Mythology any of the older gods who preceded the Olympians and were the children of Uranus (Heaven) and Gaia (Earth). Led by Cronus, they overthrew Uranus; Cronus' son, Zeus, then rebelled against his father and eventually defeated the Titans.
(as noun titan) a person or thing of very great strength, intellect, or importance: a titan of American industry.
2. Astronomy the largest satellite of Saturn (diameter 5150 km), the fifteenth closest to the planet, discovered by C. Huygens in 1655. It is unique in having a hazy atmosphere of nitrogen, methane, and oily hydrocarbons.

Contents

- 1 Preliminaries** **6**

- 2 Mission Log** **7**
 - 2.1 06:15 UTC till 10:00 UTC - Preparation in Mission Base and Trip to Launch Site 7
 - 2.2 10:00 UTC till 10:57 UTC - Launch Site Preparation 7
 - 2.3 10:57 UTC till 14:14 UTC - Tracking 9
 - 2.4 14:15 UTC - Recovery 9

- 3 Equipment Operation Review** **10**
 - 3.1 Flight Computer, GPS and Transmission 10
 - 3.2 Image Capturing 10
 - 3.3 Sensors 11
 - 3.4 Flight Control Centre 11
 - 3.5 Flight Characteristics 11
 - 3.5.1 Ascent 13
 - 3.5.2 Descent 14

- 4 Flight Path** **15**
 - 4.1 Flight Path Comparison 15
 - 4.2 Flight Velocity and Direction 19

- 5 Tracking** **20**

- 6 Image Analysis** **22**
 - 6.1 Moon 22

6.2	Balloon Burst	24
6.3	Cloud	24
7	Sensed Parameters	25
7.1	Temperature	25
7.2	Relative Humidity	27
7.3	Pressure and Altitude	28
8	Payload Motion	29
9	Conclusion	33
A	Diagrams of Raw Logged Data	34
A.1	Flight Computer Data	34
A.2	GPS Location	35
A.3	Check Status GPS	36
A.4	Luminosity, Temperature and Relative Humidity Sensor	37
A.5	External Pressure Sensors Readings	38
A.6	Precision Temperature Sensor	39
A.7	Internal Pressure Sensor Readings	40
A.8	Gyroscope Sensor Readings	41
A.9	Accelerometer Sensor Readings	42
A.10	Magnetometer Sensor Readings	43
A.11	Roll, Pitch and Heading	44

1 Preliminaries

All mission goals were accomplished with success!



Figure 1: Titan 1 looking approximately North positioned at (lat°, lon°): 55.462907, 11.311724, altitude 35 393 m at 13:27:37 UTC.

Titan 1 flew to a peak altitude of 35 393 m taking pictures and sensing the earth atmosphere and magnetic field, while transmitting constantly its position and flight computer status. An impression of the view at peak altitude gives Fig. 1.

Launch was at 10:56:51 UTC and touched down at 13:54:45 UTC leading to a total flight time of 2 h 57 min 54 s.

The following report discusses the mission regarding flight path prediction, flight performance, equipment operation and some data analyzation of the sensed data.

In appendix [A](#) the raw data of the individual sensors and the GPS position as well as the flight computer status are shown.

2 Mission Log

2.1 06:15 UTC TILL 10:00 UTC - PREPARATION IN MISSION BASE AND TRIP TO LAUNCH SITE

Before driving to the launch site all system were checked at the mission base. Especially transmission, power and image capturing. After the checks Titan 1 was assembled and packed to be ready for transport to launch site. The total weight of the payload with lines and parachute was checked resulting to 729 g, thus 9 g more than the design.

Further, a new prediction of the flight path was done to see possible deviations air traffic control should be informed about.

After packing all the individual parts, strictly following the checklists, the launch team drove to the launch site and arrived before the target time of 10:00 UTC.



Figure 2: Titan 1 and equipment prepared for balloon inflation and launch.

2.2 10:00 UTC TILL 10:57 UTC - LAUNCH SITE PREPARATION

On the launch site it was realised that the ground winds were quite strong in the order of $>5 \text{ ms}^{-1}$ with strong gusts. Thus, it was decided to inflate the balloon in the lee side of the car to gain some protection especially from the gust.

The first step was to call air traffic control to confirm flight operation. After air traffic

control stated free to go, the equipment was unpacked and everything prepared for balloon inflation and launch. Fig. 2 shows Titan 1 after startup and with hatch already sealed. Before sealing the hatch transmission and image capturing was checked carefully.

The strong wind gust made the inflation of the balloon very difficult. Not only was it difficult to hold the balloon stable and away from obstacles, but a lot of care had to be taken in order to distinguish balloon lift from air drag lift.

All pre flight operation could be concluded on 10:50 UTC and Titan 1 was ready for launch, see Fig. 3.



Figure 3: Titan 1 shortly before launch in a calm wind moment.

Due to the very strong winds it was decided to not risk damage to the balloon and launched slightly before time at 10:56:51 UTC.

2.3 10:57 UTC TILL 14:14 UTC - TRACKING

10:56:51 UTC Titan was successfully launched and started heading for the peak altitude, see Fig. 4. While Titan 1 was flying the launch team moved to **Wait** position (see Fig. 10) to have lunch and continuously track Titan 1.



Figure 4: Titan 1 shortly after launch at an altitude of approximately 200 m.

2.4 14:15 UTC - RECOVERY



Figure 5: Titan 1 on landing site before recovery. Head of mission is talking to air traffic control to confirm touchdown and recovery.

At 14:03:57 UTC Titan 1 was spotted after tracking it from search position **S1** (see Fig. 10) and moving to search position **S2** (see Fig. 10). Titan 1 landed in a recently harvested field and could luckely be recovered with ease.

3 Equipment Operation Review

The following section gives a critical review of all components of Titan 1. Especially expected operation and functionality are discussed in relation to observed behaviour.

3.1 FLIGHT COMPUTER, GPS AND TRANSMISSION

The flight computer operated throughout the mission without any problems. As the logged values for *count* in Fig. 28 confirm. In the same figure *battvaverage* is shown which proves that the power source was designed with good reserves, voltage drop is mostly due to temperature decrease. Flight computer minimum logged temperature (*temperature1*) was -2°C .

Data logging was operational throughout the whole mission, see Fig. 28 Logging to micro-SD Status.

GPS was nominal during whole mission, see Fig. 29 and Fig. 30. An important point is the smooth transmission from pedestrian to flight mode.

Transmission was excellent during the whole flight and also after touchdown. The transmission frequency was very stable as no major frequency shift could be observed. Some more details about tracking gives section 5.

3.2 IMAGE CAPTURING

The GOPro camcorder worked perfectly from mission start to recovery thanks also to the Battery BacPac providing enough extra power. However, the idea of filling the housing with Dust-Off (1,1-Difluoroethane) did not work as expected. During ascent from approximately 3177 m up to 32 777 m the lens of the housing got fogged. Little to say it was real luck that at peak altitude the lens fogging disappeared. During descent no fogging could be observed. It seems however that the defogging took place while the housing leaked and equalised with the low pressure at altitude. The housing's internal pressure was below atmospheric pressure at recovery as the housing had to be equalised before opening.

3.3 SENSORS

Apart from the luminosity sensor TSL2561 and the pressure sensor MPL3115A2 all sensors performed exceptionally well.

What caused the strange jumps and errors in the MPL3115A2 pressure and temperature readings is not fully clear. However, it looks like reading from the sensor is not done correctly, this holds particularly for the temperature reading where temperature values below zero are all ambiguous, whereas positive temperatures are shown correctly, see Fig. 32.

Tests conducted after the flight with the luminosity sensor TSL2561 resulted in following explanation for the errors readings. It seems as if too strong light hits the sensors it get saturated resulting in an ambiguous reading of 53 lx, see Fig. 31.

Before using both sensors in future mission a careful check will be conducted in order to understand operability during high altitude missions.

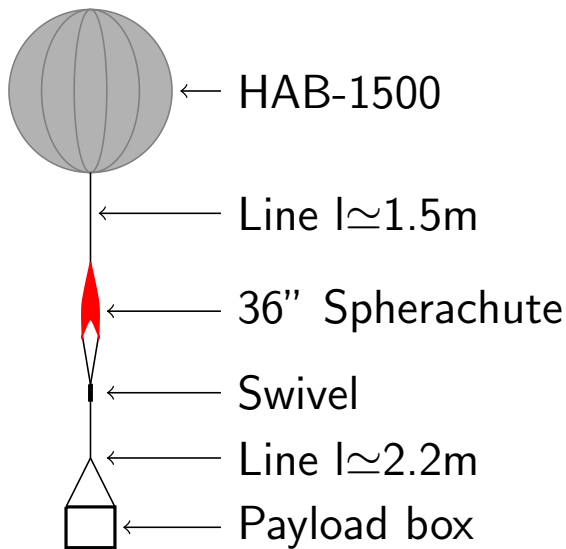
A remark has to be given on the calibration the magnetometer sensor readings. The sensor was calibrated the morning before driving to the launch site. However, (as not really surprising) the calibration is not too accurate when at the launch site. It was tried to calibrate from the raw logged magnetometer sensor readings, but leading to not satisfying results. Next time the calibration will take place on site before launch.

3.4 FLIGHT CONTROL CENTRE

During flight operation a bug was identified in the Flight Control Centre. The default variable in case the user location could not be obtained was not set properly and leading to the map to not visualise properly. Defining the variable properly solved the problem.

3.5 FLIGHT CHARACTERISTICS

Probably the most difficult part during design of a high altitude balloon is the prediction of its behaviour. In the Design and Mission Documentation the main technical characteristics of Titan 1 are stated and the most relevant parameter as per design are:



- Peak Altitude:** 35 104 m
- Ascent Velocity:** 5.59 m s^{-1}
- Descent Velocity:** 4.78 m s^{-1}
- Ascent Time:** 105 min
- Descent Time:** 122 min
- Payload Weight:** 0.720 kg
- Balloon Volume at Launch:** 3.460 m^3
- Balloon Lift at Launch:** 3.548 kg

As relevant to better understand the individual sensor readings, a schematic view of the payload box is shown in Fig. 6. Of special importance is the coordinate system of the IMU sensor.

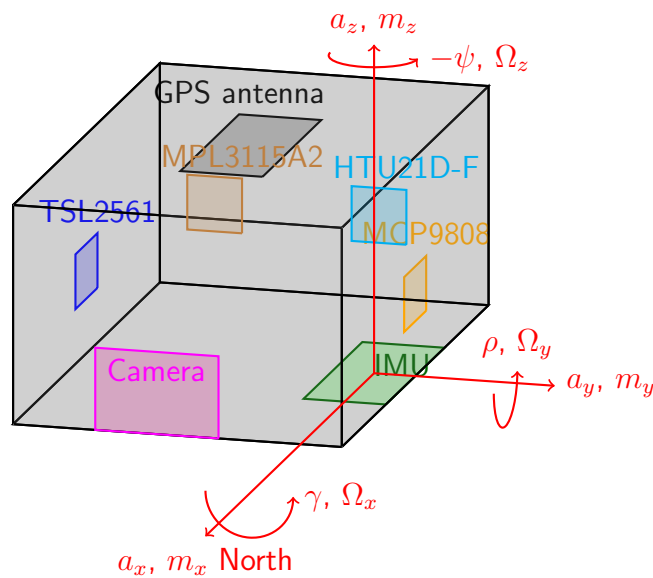


Figure 6: Schematic of payload box with sensor location and coordinate system of the IMU sensor.

Based on the GPS altitude $maxalt$ the vertical velocity was calculated, see Fig. 7. For the plot the coordinate convention as defined in the Design and Mission Documentation was used, ascent movement positive, decent movement negative, see coordinate system in Fig. 6.

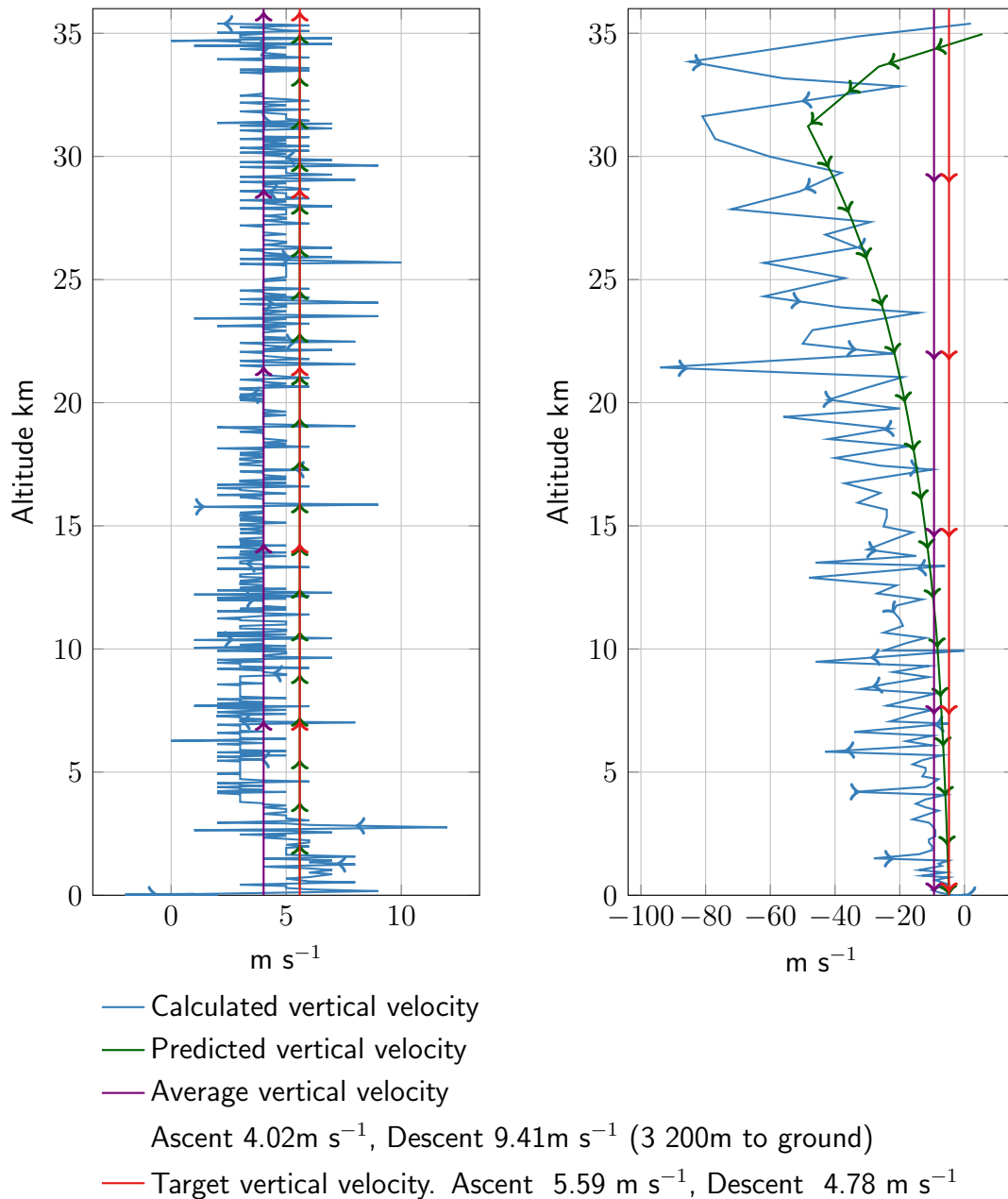


Figure 7: Vertical velocity during ascent (plot on the left) and during descent (plot on the right) calculated from GPS altitude.

3.5.1 Ascent

The average ascent velocity results in 4.02 m s^{-1} which is a factor 0.72 smaller than the design velocity of 5.59 m s^{-1} . Leading to an ascent time of 151 min (logged value) instead of the calculated 105 min, 46 min longer. As the payload weight was only marginal larger than the design value the (9 g more) the difference is most likely caused by a less inflated balloon, i.e. lower fill volume V_L .

Back calculating with the formula for the burst altitude

$$H_B = -\frac{RT_B}{gM} \ln \left[\frac{d_{L,real}^3}{d_B^3} \right] = -\frac{RT_B}{gM} \ln \left[\left(\frac{d_{L,real}}{9.45m} \right)^3 \right] = 35393m, \quad (1)$$

results in $d_{L,real} = 1.740m$ with T_B estimated as 238.15 K. All other values kindly see Design and Mission Documentation. The launch volume results in

$$V_{L,real} = \frac{4}{3} \pi \left(\frac{d_{L,real}}{2} \right)^3 = \frac{4}{3} \pi \left(\frac{1.740m}{2} \right)^3 \approx 2.756m^3. \quad (2)$$

The balloon volume at launch was designed to be 3.460 m³ which is 1.25 times more. Thus the real balloon gross lift $G_{L,real}$ at launch is

$$G_{L,real} = \rho \frac{4}{3} \pi \left(\frac{d_{Lr}}{2} \right)^3 = 1.0255kgm^{-3} \cdot 2.756m^3 = 2.827kg \quad (3)$$

and thus the free lift $F_{L,real}$

$$F_{L,real} = (G_{L,real} - m_P - m_B) g = (2.827kg - 0.729kg - 1.500kg) g = 5.86N. \quad (4)$$

The ascent velocity $v_{a,real}$ results to

$$v_{a,real} = \sqrt{\frac{2 F_{L,real}}{C_d \rho_{Air} \pi (d_{L,real}/2)^2}} = \sqrt{\frac{2 \cdot 5.86N}{0.25 \cdot 1.2041 \cdot \pi (1.740m/2)^2}} = 4.05ms^{-1}, \quad (5)$$

which correspond perfectly to the average ascent velocity of 4.02 m s⁻¹.

3.5.2 Descent

The average descent velocity is 9.41 m s⁻¹, which is 1.97 times larger than the calculated descent speed of 4.78 m s⁻¹. The descent time was 27 min instead of the calculated 122 min, thus 95 min shorter. This is as such not suppressing as the average descent velocity is more like a target touchdown velocity and as such only true for the last couple of hundred meters above ground.

The faster descent is caused partly by the additional weight of the remains of the burst balloon m_B which is 920 g and the fact that the lines got wrapped around the parachute's line, see Fig. 8. When looking at Fig. 7 it becomes clear that the descent velocity (not surprisingly) reduced as more Titan 1 descent into denser atmospheric layers. Thus, the average descent velocity is taken only for 3200 m altitude to ground.

Estimating the descent velocity $v_{d,real}$ with reduced parachute opening diameter $d_{P,real}$ leads to

$$v_{d,real} = \sqrt{\frac{2 (m_P + m_B) g}{C_{d,P} \rho_{Air} \pi (d_{P,real}/2)^2}} = \sqrt{\frac{2 \cdot (0.729 + 0.920) \cdot g}{0.78 \cdot 1.2041 \cdot \pi (0.700m/2)^2}} = 9.46ms^{-1}. \quad (6)$$

The parachute opening diameter $d_{P,real}$ was chosen with 0.700 m to fit the average descent velocity of 9.41 m s^{-1} . Comparing with the parachute opening in Fig. 8 the value seems about correct. Some more discussion regarding descent behaviour is given in section 8.



Figure 8: Titan's parachute with balloon remains wrapped around the parachute's lines. This image proves that the parachute opened during descent, even if not fully.

4 Flight Path

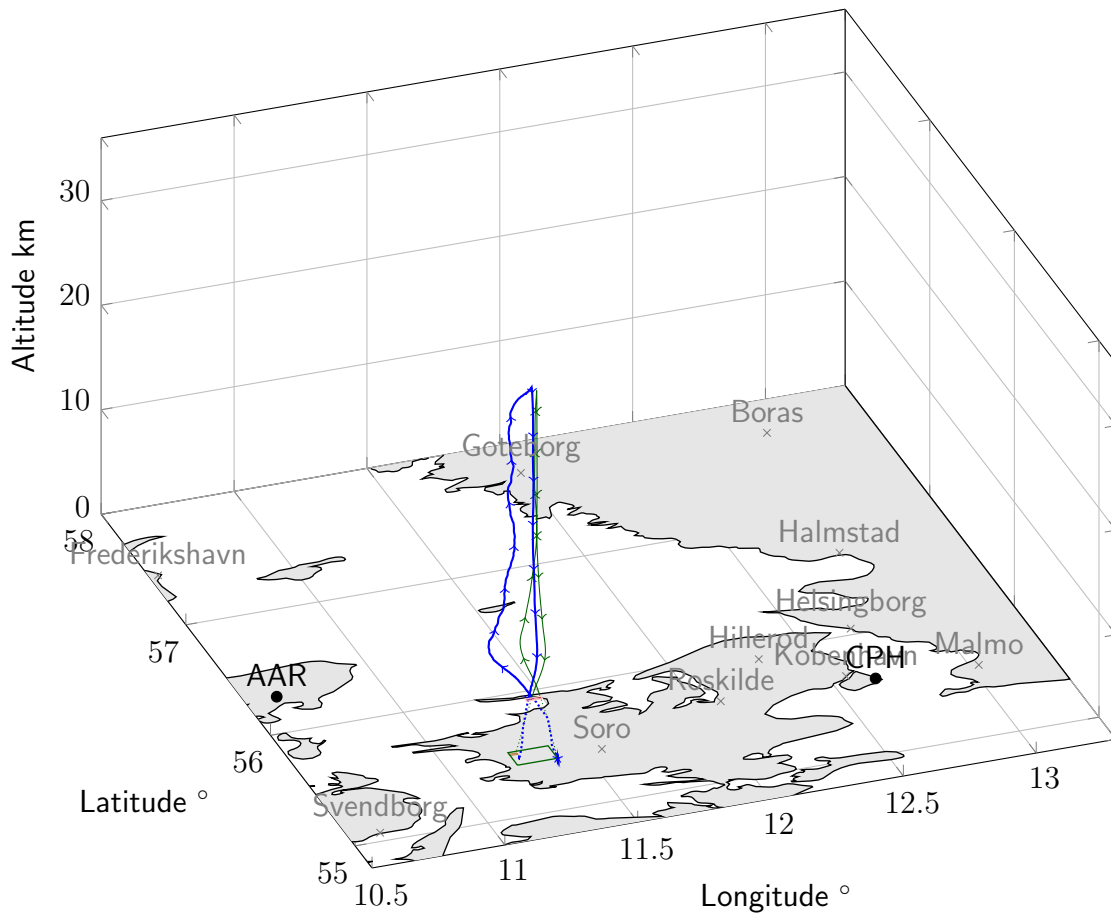
Following paragraph discussed the the flight path of Titan 1 especially in comparison with the prediction made prior to the flight. Further, the flight direction and velocity is discussed, see section 4.2.

4.1 FLIGHT PATH COMPARISON

In section 3.5.1 the ascent velocity and in section 3.5.2 the descent velocity were discussed. These two values are fundamental in order to understand deviations from the flight path documented in Fig. 9, Fig. 10 and Fig. 11.

Staring with Fig. 10 allows to get a fast inside into what caused deviations from the

perdition to the actual flight path. As the balloon ascent much slower the ground winds dragged the balloon much farer north west. Notice however, how well the direction is aligned between prediction and flight path, see Fig. 12.



- × Major cities
- Major danish airports
- * Launch site (lat°, lon°): 55.4204, 11.3964
- Titan 1 flightpath prediction +24h, below 18000ft
- Titan 1 flightpath prediction +24h, above 18000ft
- Titan 1 flightpath, below 18000ft
- Titan 1 flightpath, above 18000ft
- 18000ft penetration zone (rect. lat°, lon°): 55.459, 11.292 / 55.480, 11.352
Penetration time ascent: between 11:15:00 UTC and 11:18:20 UTC
Penetration time descent: between 12:50:00 UTC and 13:32:30 UTC
- Estimated touchdown zone (rect. lat°, lon°): 55.507, 11.245 / 55.519, 11.274
Touchdown time: between 13:04:53 UTC and 13:51:30 UTC
- Area of flight operation (rect. lat°, lon°): 55.420, 11.245 / 55.533, 11.396

Figure 9: Isometric view of real flight path and predicted flight path. For reference all details send to the air traffic control are included as well.

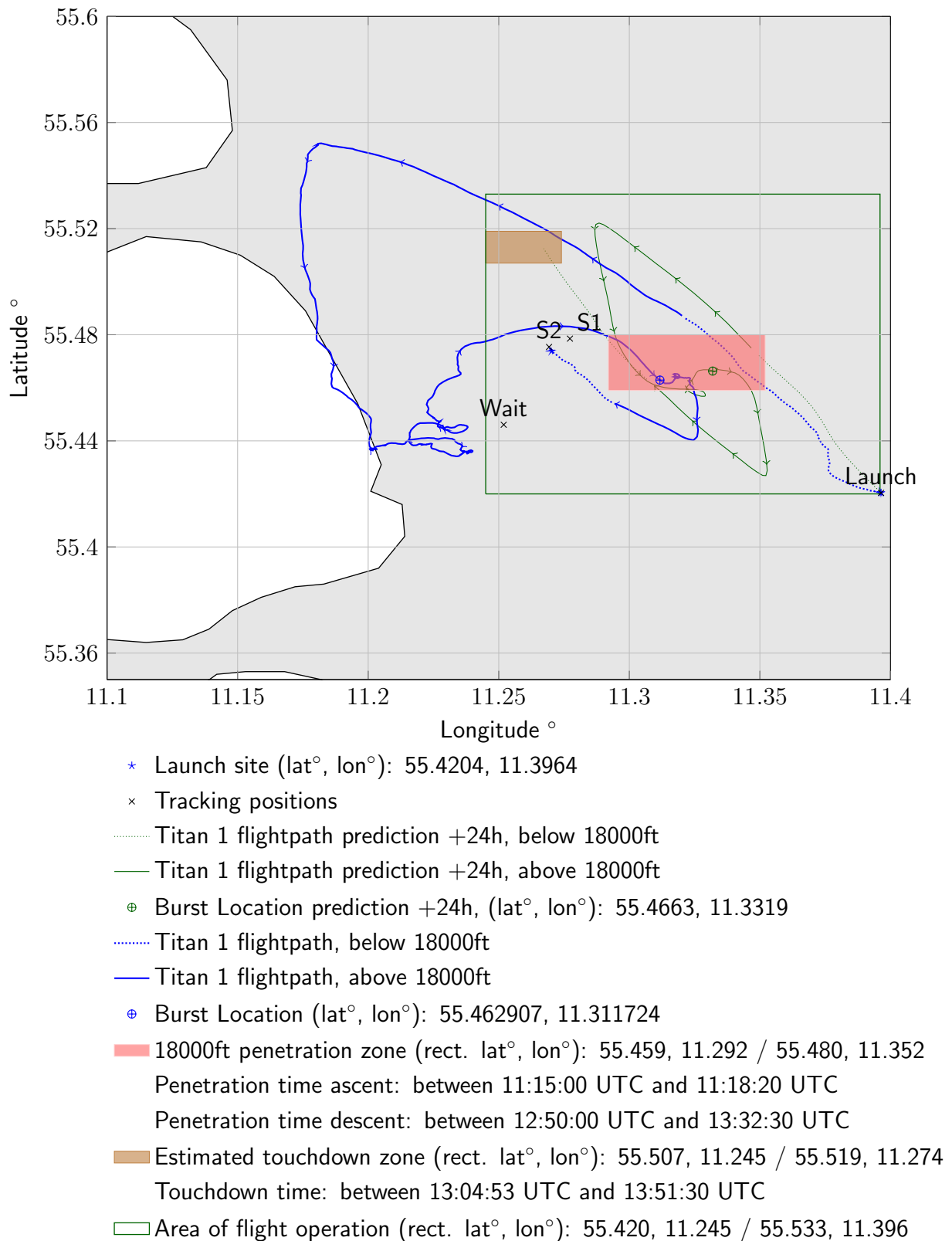


Figure 10: Top view of real flight path and predicted flight path. For reference all details send to the air traffic control are included as well and the tracking positions.

Once reaching around 10 000 m, see also right plot in Fig. 11, the jetstream drags the

balloon nearly straight south. Again farer as the prediction as the balloon remains longer in the altitude range of the jet stream. Once above the jetstream the balloon movement is characterised by small high atmosphere movements dragging Titan 1 west east, especially above 30 000 m. See again Fig. 11 right plot were this observation becomes clear. What we can see is that the burst location is very near to the predicted burst location, see Fig. 10.

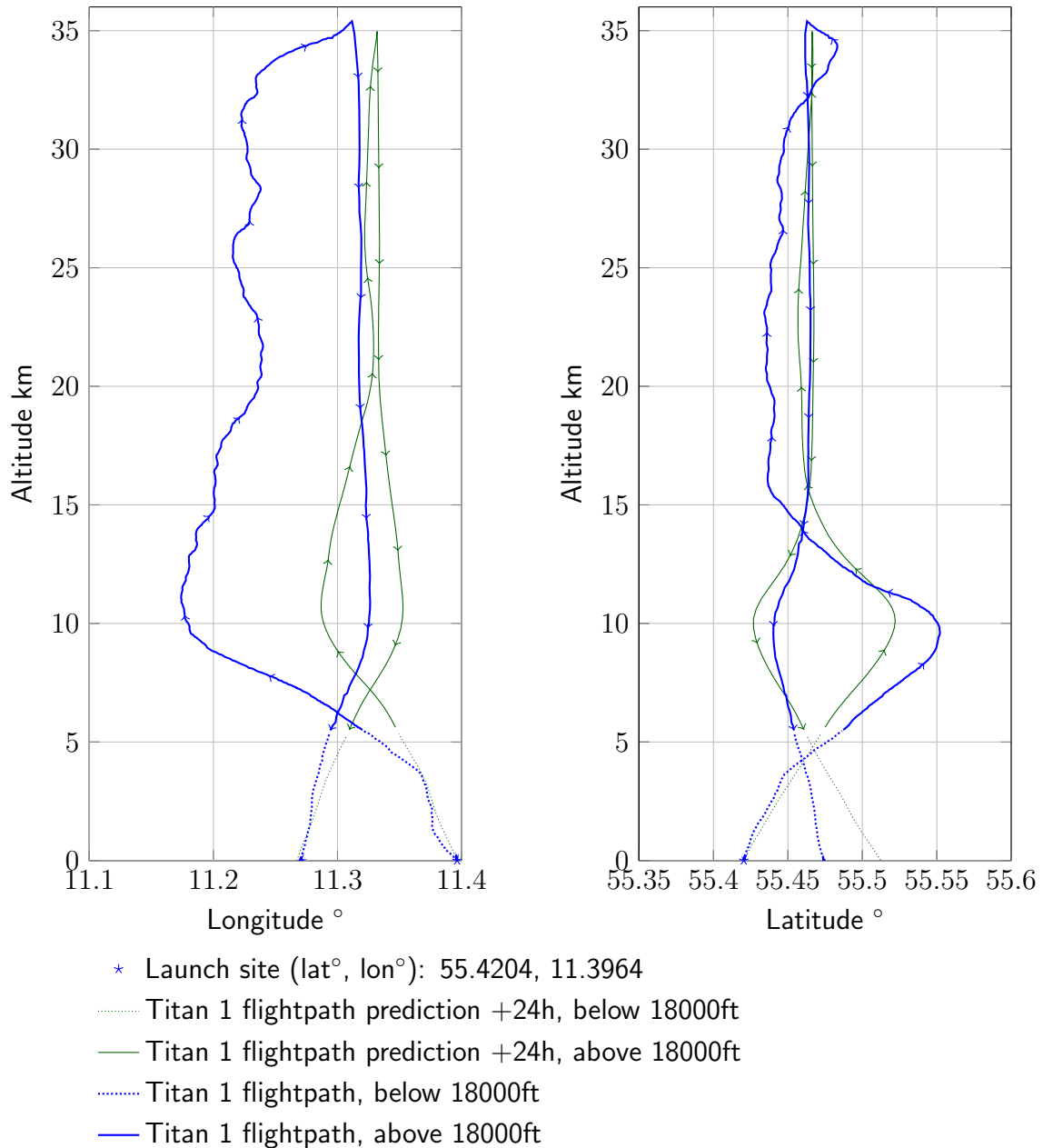


Figure 11: Side view of real flight path and predicted flight path.

After the balloon bursted, it dropped more or less vertically till reaching the jetstream again, which is good in line with the prediction. This time the vertical speed is much faster and thus, the jetstream does not drag the balloon as fare as predicted. Same holds for the flightpath below the jetstream. Additional the wind direction is more westerly

than in the prediction, see Fig. 13. This lead to Titan 1 touchdown more south than predicted.

4.2 FLIGHT VELOCITY AND DIRECTION

Fig. 12 and Fig. 13 show very good agreement between the predicted Titan's fly velocity (Speed over Ground) and direction. As a comparison in terms of altitude takes the time out, this only proofs that the predicted wind velocity and direction for all altitude are considerable exact. Some smaller deviations can be found at altitudes above 25 000 m during ascent.

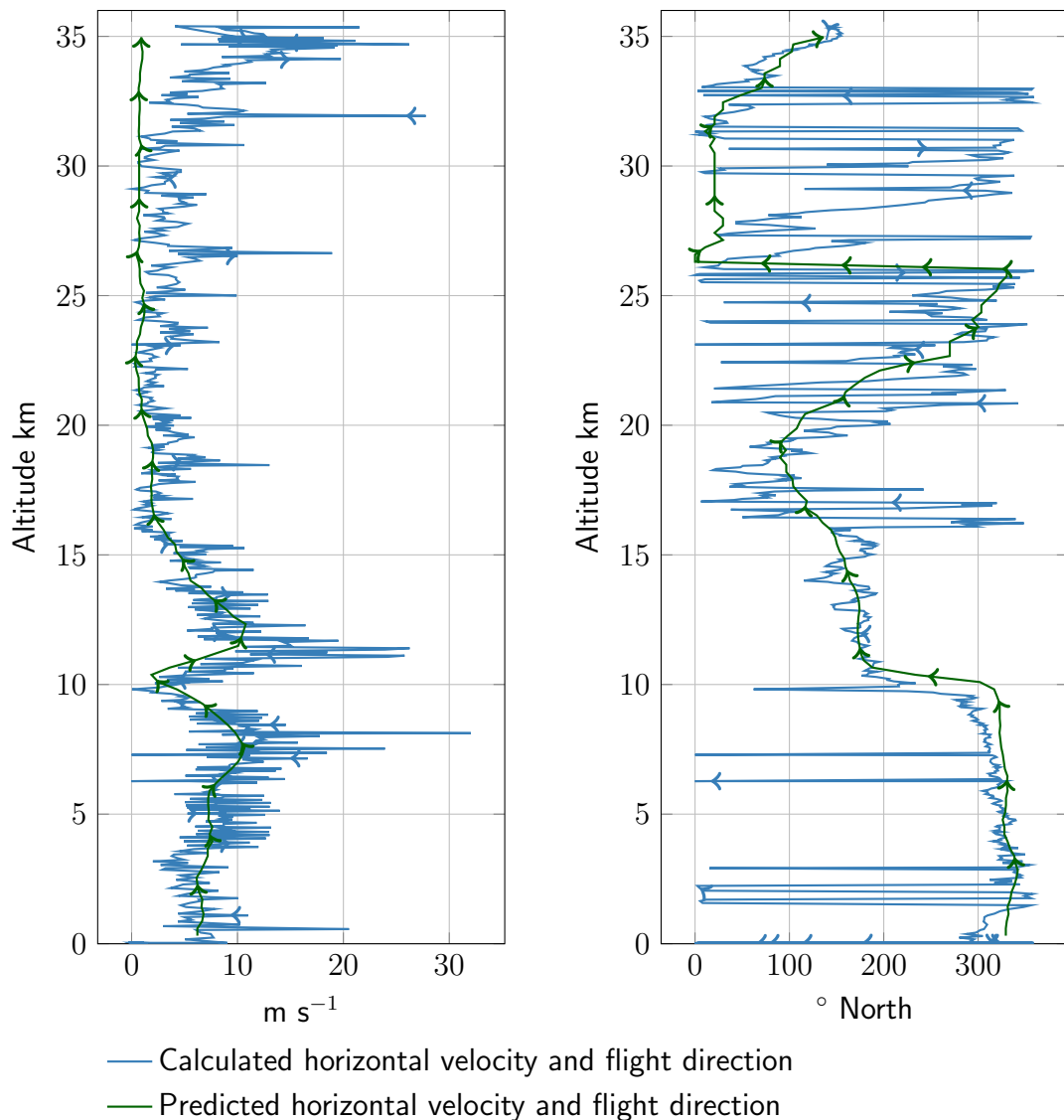


Figure 12: Horizontal velocity and direction of Titan 1 during ascent. For comparison also the predicted velocity and direction are shown.

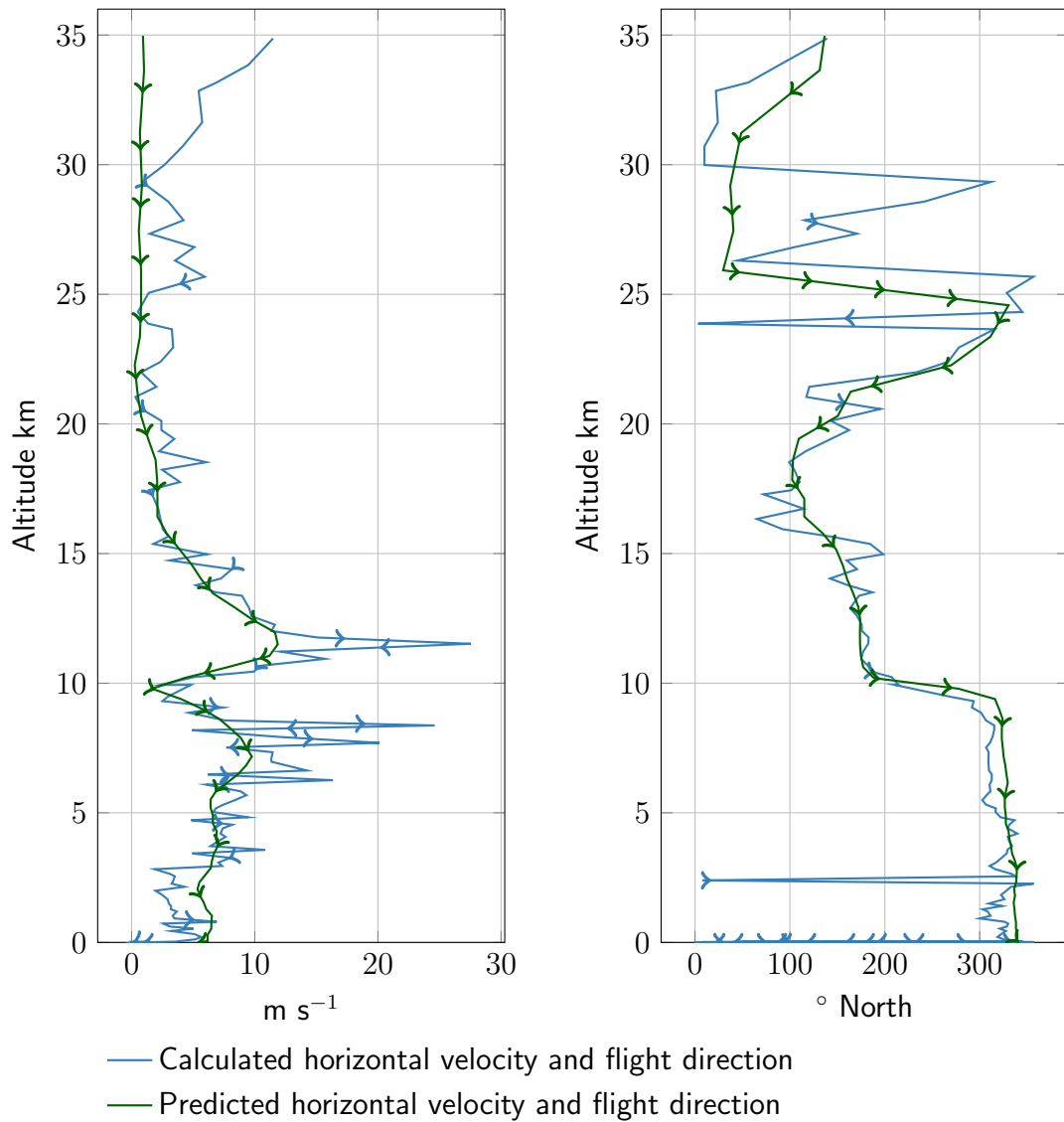


Figure 13: Horizontal velocity and direction of Titan 1 during descent. For comparison also the predicted velocity and direction are shown.

5 Tracking

The flight was tracked constantly by the launch team and following persons:

SA6BSS Slutarp, Sweden. Ground distance approximately 327 km.

DL1SGP Lachendorf, Germany. Ground distance approximately 333 km.

OZ1SKY Skodstrup, Denmark. Ground distance approximately 116 km.

Which should again be thanked for their effort feeding the received data into <http://tracker.habhub.org/>.

Fig. 14 shows the logged flight path and the positions tracked by the individual trackers. The positions of the launch team are shown as well for reference.

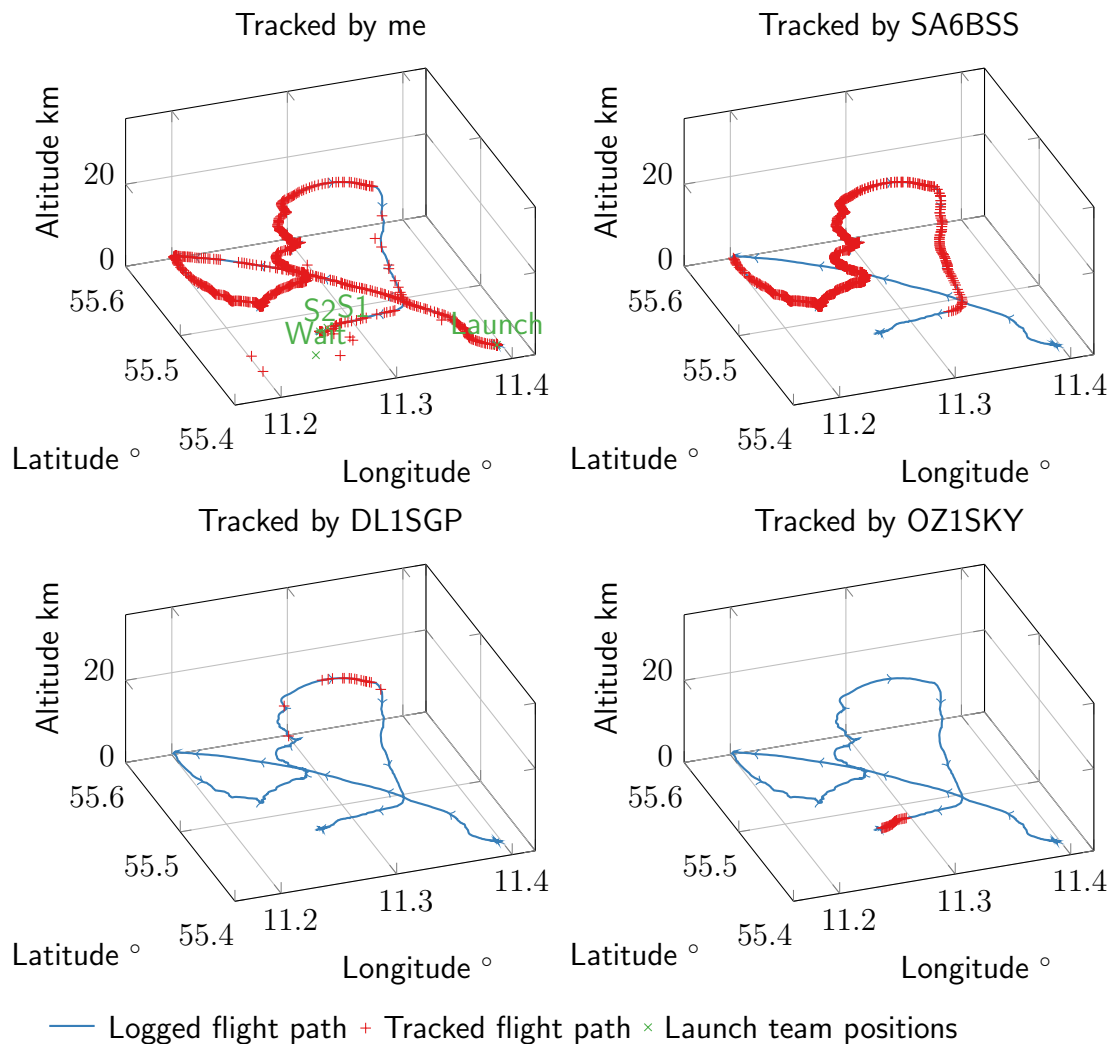


Figure 14: Logged flight path with tracked flight path of Titan 1. Plots are shown individually for the four trackers.

The launch team was able to track the flight constantly except for some short moment while moving from **Launch** position to the **Wait** position and while moving to the touch-down location, search position **S1** and **S2**. This mostly due to holding the antenna out of the window while diving does not allow to have good contact all the time.

Looking at the tracked points by SA6BSS in Fig. 14 shows that the contact horizon was at approximately 7933 m. Above that level the tracking was constant. DL1SGP had a good spot on during the peak approach of Titan 1. OZ1SKY only tracked the final touchdown path of the flight down to 210 m above ground.

The signal was very stable and no frequency shifting has been observed, which was also confirmed during the flight by SA6BSS and DL1SGB.

6 Image Analysis

During the flight an images was taken every second leading to a total amount of 11 489 images taken from shortly before launch up to shortly after recovery. An infinity amount of images could be shown and discussed here, but the author wanted to concentrated on the few most impressive images.

6.1 MOON

On August 21th 2015 the moon could not be seen from earth surface as the light was to bright. However, once up it could easily be seen, see Fig. 15 and Fig. 16. That day the moon raised at 11:20 UTC and set on 16:13 UTC. The moon was waxing crescent at 38 % and had a moon age of 6.2 days.

At 11:23 UTC when Fig. 15 was taken the moon was at a distance of 398 887 km at an elevation angle (from ground) of 13.42° and an azimuth angle of 139.59° . Titan 1 was at an altitude of 32 834 m.

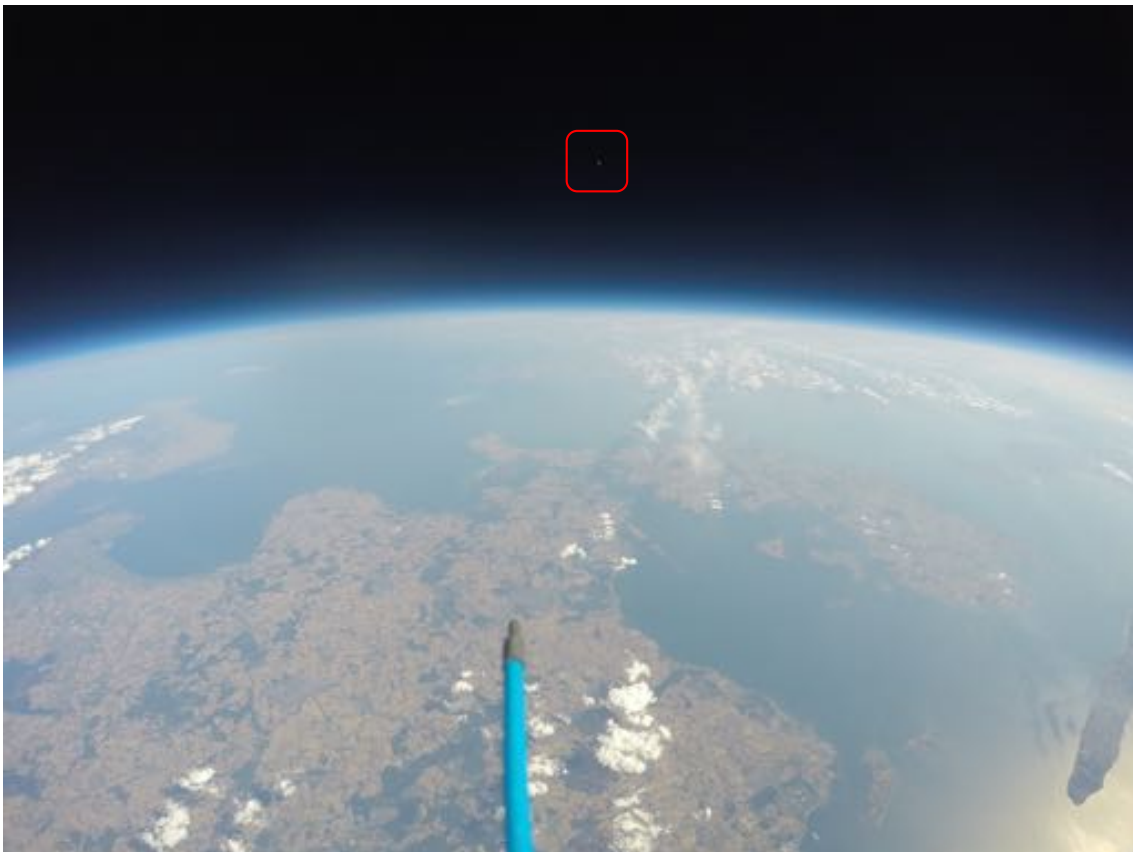


Figure 15: Titan 1 at 32 834 m looking approximately 135° North at 13:16:10 UTC. Inside the red square is the moon.

Fig. 16 was taken at an latitude of 35 349 m with the moon standing at a distance of 398 887 km at an elevation angle (from ground) of 13.45° and an azimuth angle of 139.66°.

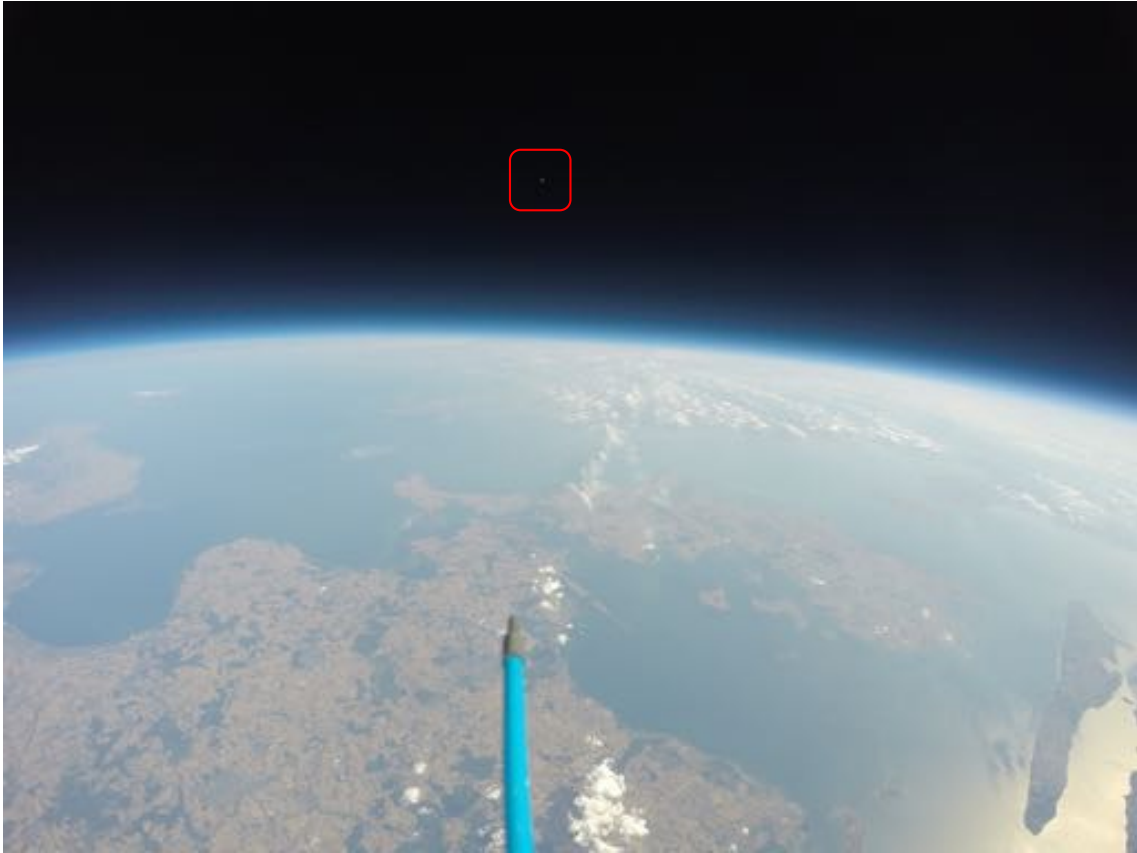


Figure 16: Titan 1 at 35 349 m looking approximately 139° North at 13:27:25 UTC. Inside the red square is the moon.



Figure 17: Magnification of the moon in Fig. 16. Remarkable is the darkness of space due to low light sensitive of the camcorder.

Fig. 17 shows a magnification of the moon as seen in Fig. 16. The waxing crescent of the

moon can be nicely observed. The resolution of the image is impressive, remember the distance to the moon is 398 887 km, as still the moon's dark spots can be identified.

6.2 BALLOON BURST

The second major event, after the launch, is when the balloon bursts at peak altitude. The first image taken after the balloon's burst is shown in Fig. 18. Titan 1 ended up upside down before returning in normal flight position.



Figure 18: First image taken after burst of the balloon, Titan 1 ending upside down. Some fragments of the balloon can be seen. Image taken at 13:27:38 UTC.

6.3 CLOUD

Clouds, known for the particular beauty, should not be missed out, see Fig. 19. Titan 1 penetrated through clouds during ascent, but through even more intense clouds during descent. The image is taken at an altitude of 2825 m. The sun stands at 228.95° North at an elevation angle (from ground) of 37.83° . The clouds seem to be of the altocumulus type.



Figure 19: Titan 1 penetrating through the altocumulus cloud layer during descent at 13:49:28 UTC, altitude 2825 m.

7 Sensed Parameters

This section states and discusses in short the measured atmospheric parameters temperature, relative humidity and pressure as well as the measured values for the magnetic field.

7.1 TEMPERATURE

Fig. 20 shows the external (atmospheric) and internal temperature. The external temperature is a little above of what would have been expected (minimum around -50°C) is probably due to the fact the sensors being exposed to sun light. In a future mission the sensors will be mounted without direct light impact. The internal temperature follows the external temperature with a time delay. The minimum flight computer is logged with -2°C .

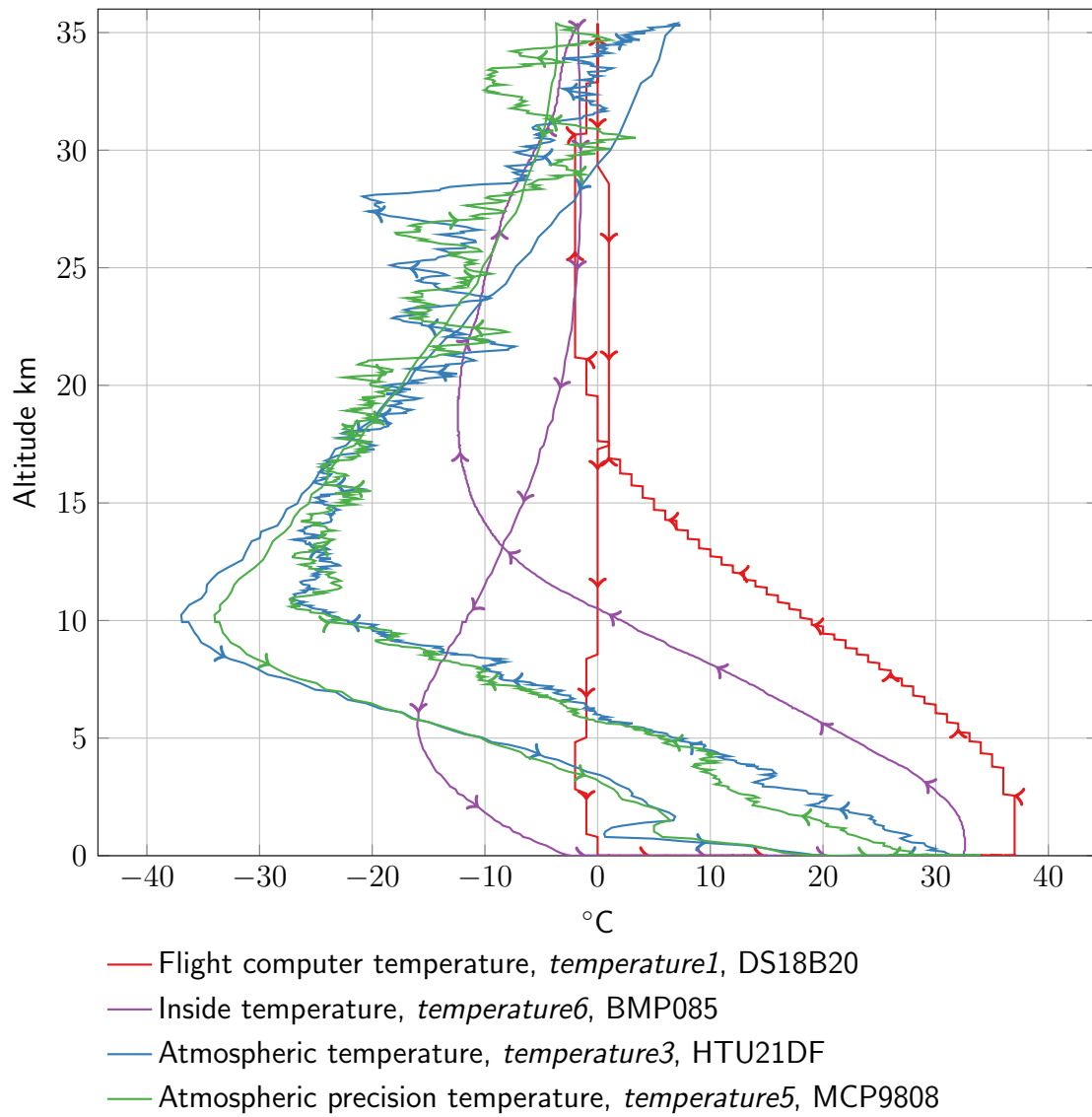


Figure 20: Temperature readings for different temperature sensors inside the payload box and on the outside.

7.2 RELATIVE HUMIDITY

The relative humidity of the atmosphere is measured with the HTU21DF sensor and results are shown in Fig. 21. The values are not corrected for the reduced pressure in altitude and thus resulting in a relative humidity below zero. Interesting however is that the cloud level (around 3200 m) can be sensed by increased relative humidity.

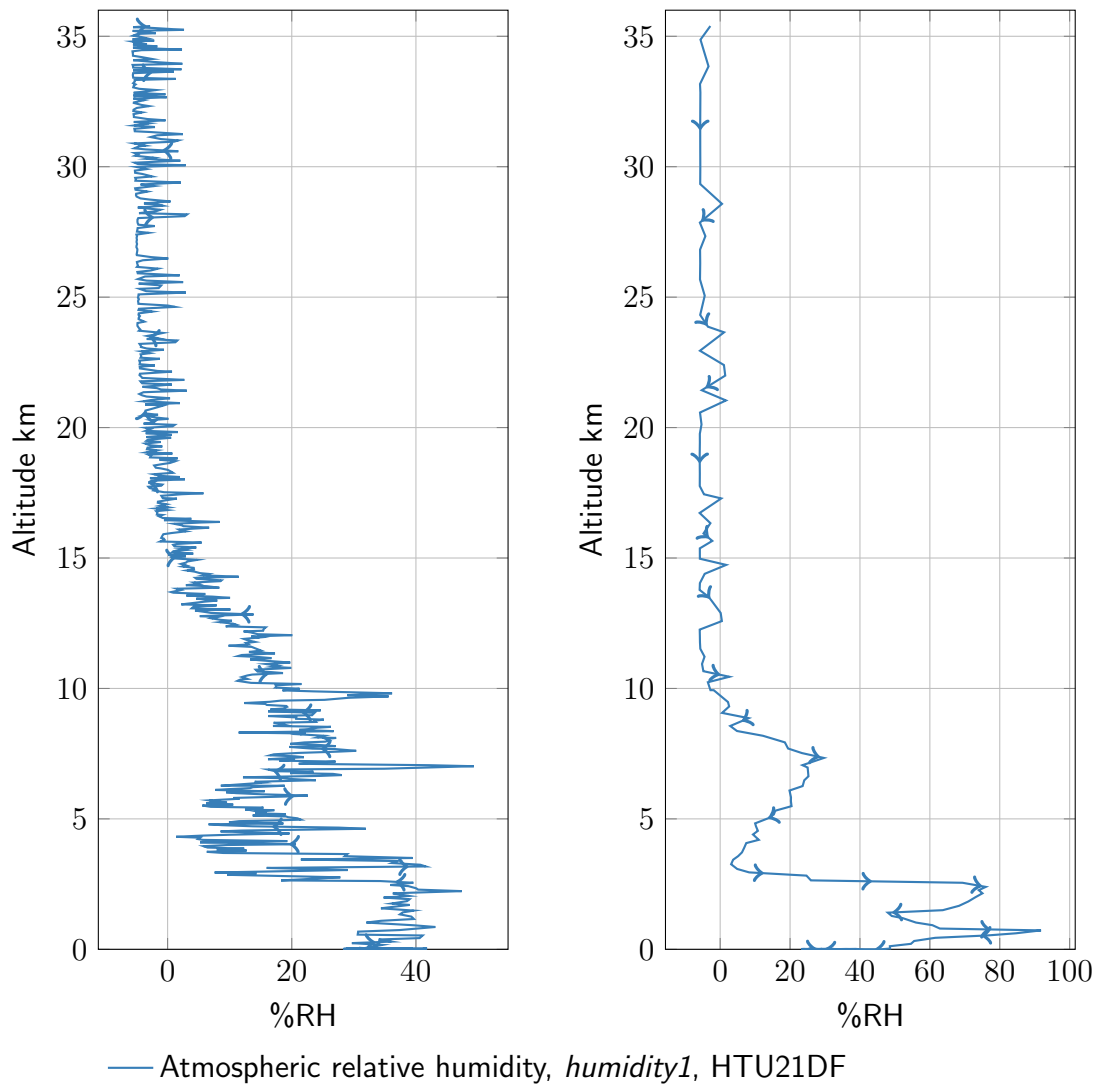


Figure 21: Relative humidity of the atmosphere without accounting for pressure correction.

7.3 PRESSURE AND ALTITUDE

The sensed pressure is shown in the left plot of Fig. 22 where as on the right plot in Fig. 22 the calculated altitude from the sensed pressure is compared with the GPS altitude. Unfortunately, the readings of the MPL3115A2 sensor are in parts ambiguous, but the indication of the pressure reduction gets clear. The BMP085 sensors gave very stable readings. However, for both sensors the atmospheric pressure gets too low (approximately 800 Pa at 35 000 m) to sense accurately. BMP085 sensor has a lower limit of 30 kPa and the MPL3115A2 sensor 20 kPa, for both much larger than the actual pressure.

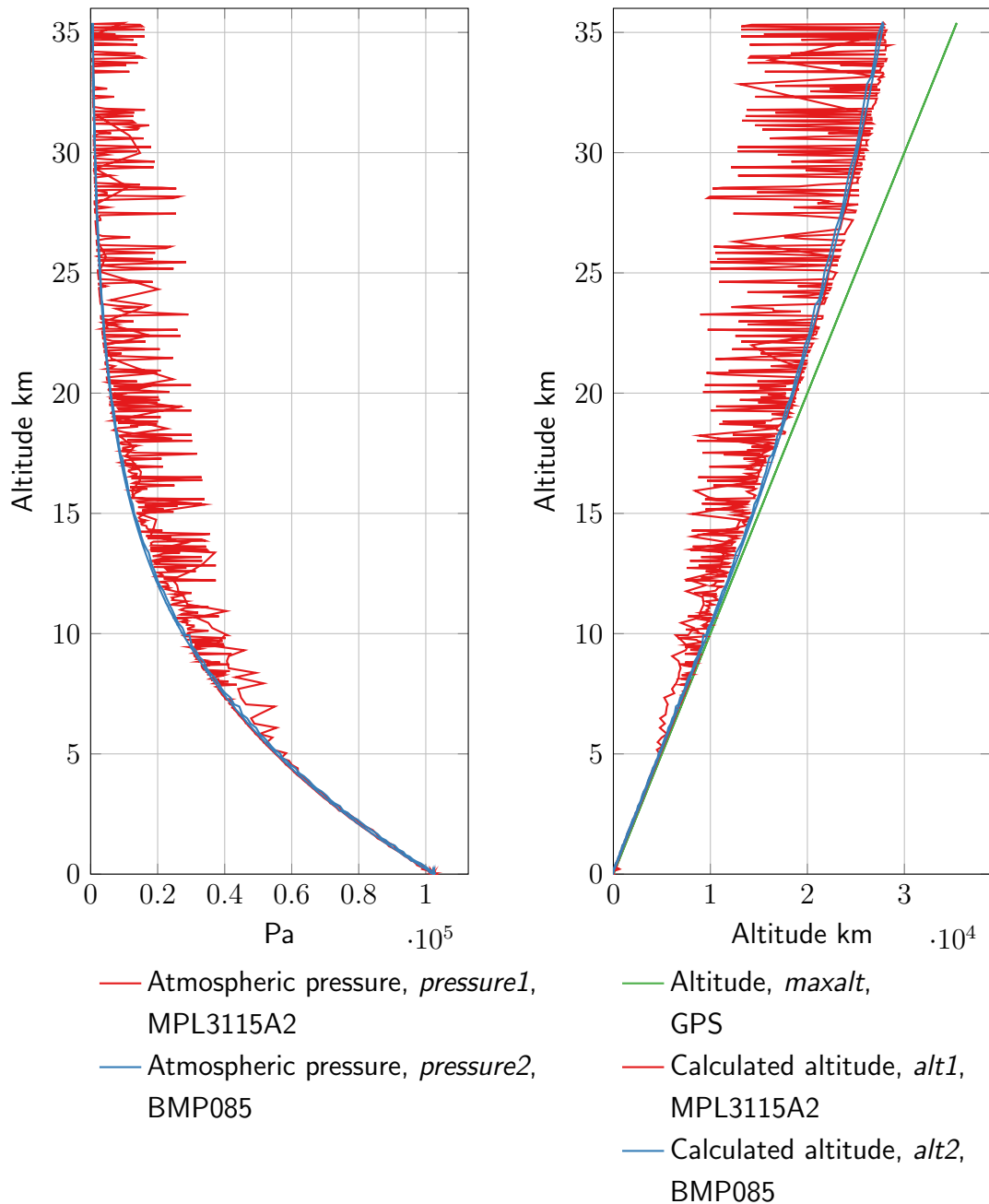


Figure 22: Pressure sensor readings and comparison of calculated altitude with actual GPS altitude.

8 Payload Motion

In this section a short investigation of the payload motion is given. The coordinate system of the IMU sensor is shown in Fig. 6. The fundamental movements are roll, pitch and heading, the relative values over hight are shown in Fig. 23, Fig. 24 and Fig. 25.

Looking at roll and pitch, it becomes clear that during ascent the payload box remained mostly horizontal. Some small mean angular deviation can be observed in Fig. 23 and Fig. 24, however it looks like they are caused by a sensor offset, see Fig. 36 as from the taken images it can be understood that the payload box was considerable horizontal.

During descent through the upper atmosphere the payload box is rolled to the left and and pitched up. I.e. the corner where the IMU sensor is located is lower than the opposite corner and the camera is looking up, see Fig. 6.

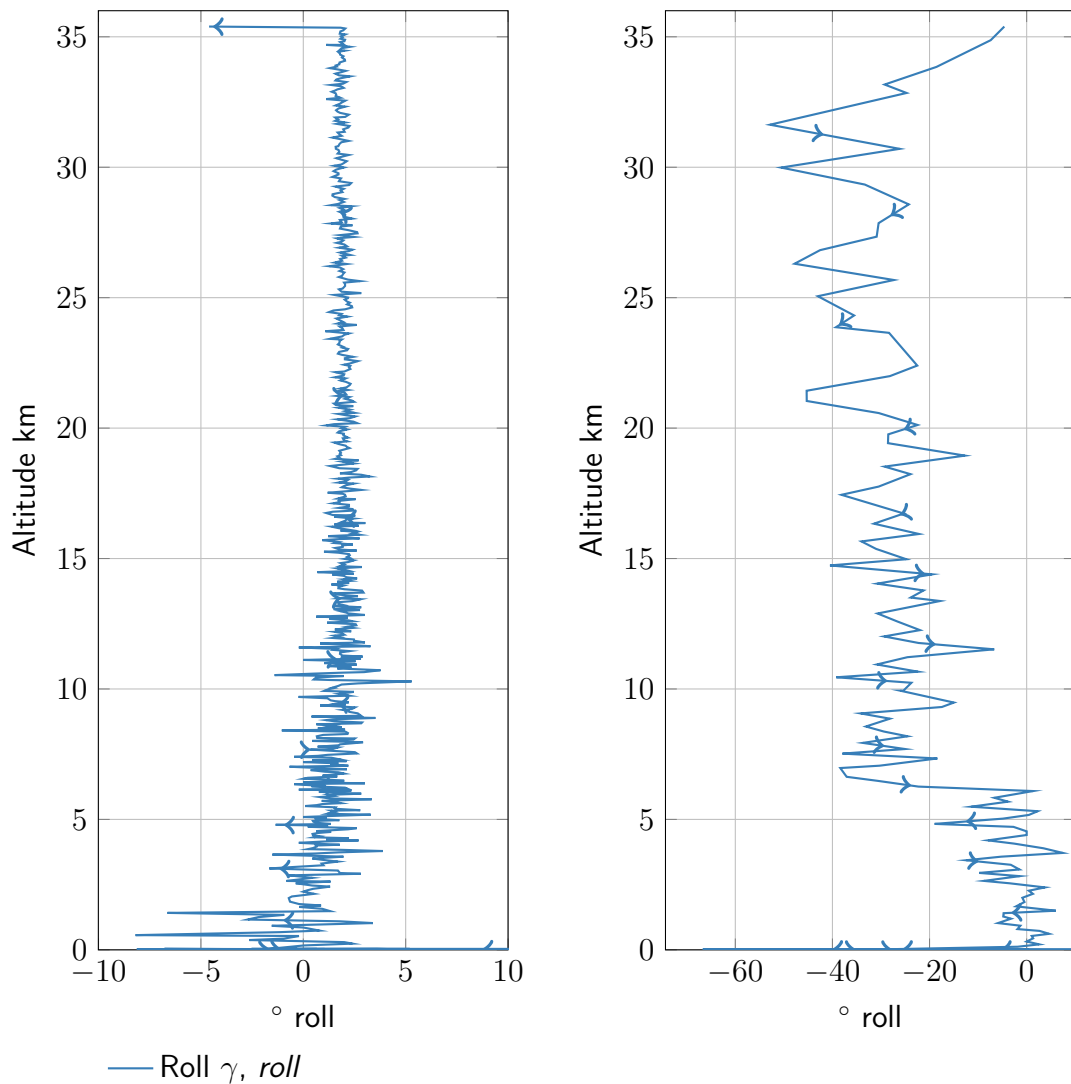


Figure 23: Roll of Titan 1's payload box during ascent and descent. Values derived from earth acceleration readings.

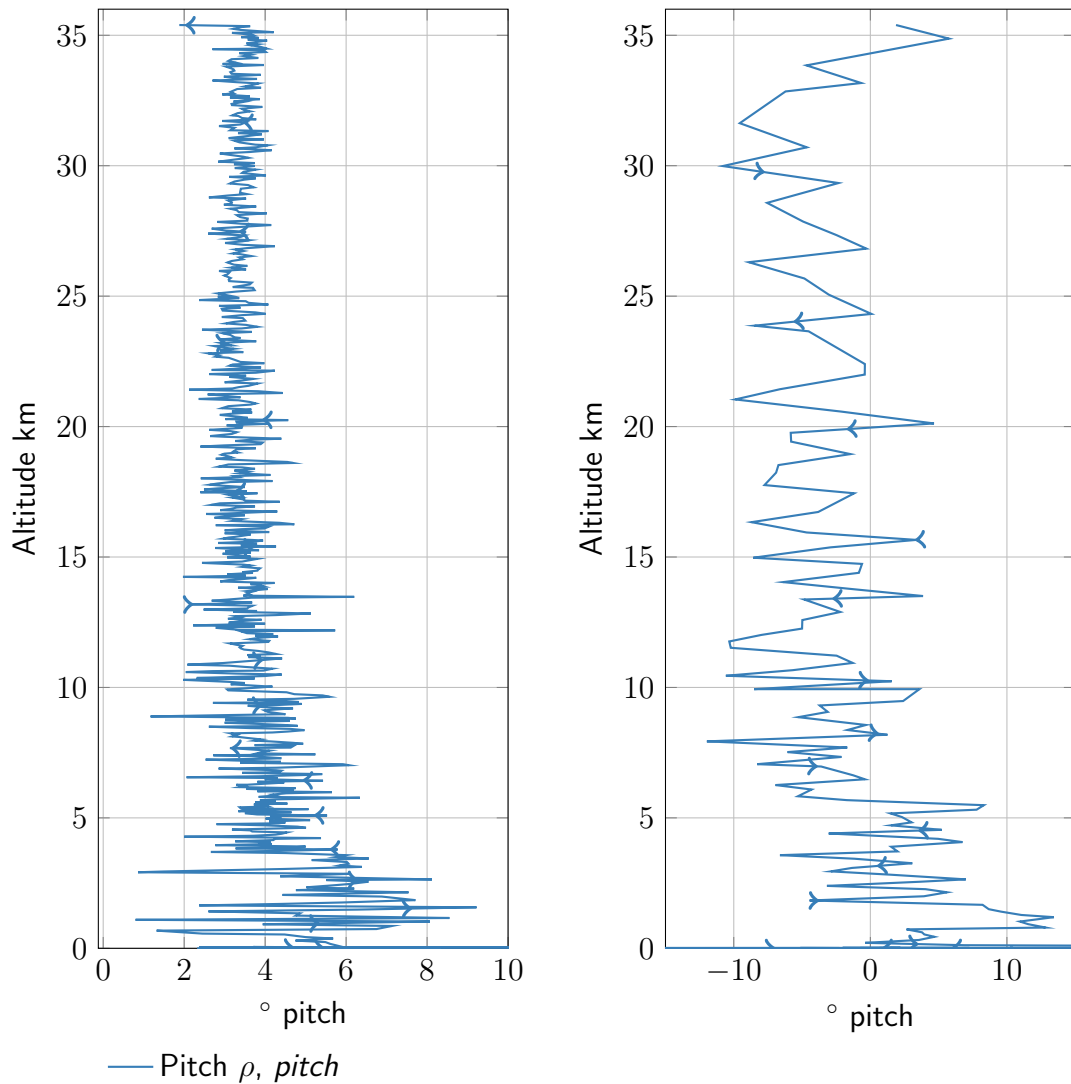


Figure 24: Pitch of Titan 1’s payload box during ascent and descent. Values derived from earth acceleration readings.

As already pointed out the calibration of the magnetic sensor was done before driving to the launch site, this lead to a poorly calibrated magnetic sensor and thus to ambiguous heading values. However, the values are shown in Fig. 25. The heading becomes more interesting when compared to the vertical payload spin, see Fig. 27. The payload box rotates more or less in one direction and then rotates back, quite strong at the beginning but once reaching high altitude the angular velocity reduces. This, somehow proofs that the installed swivel increases rotational stability (less spin is transferred form the parachute and or balloon to the payload box) of the payload box. Further, this is confirmed by analysing the images taken by the camcorder.

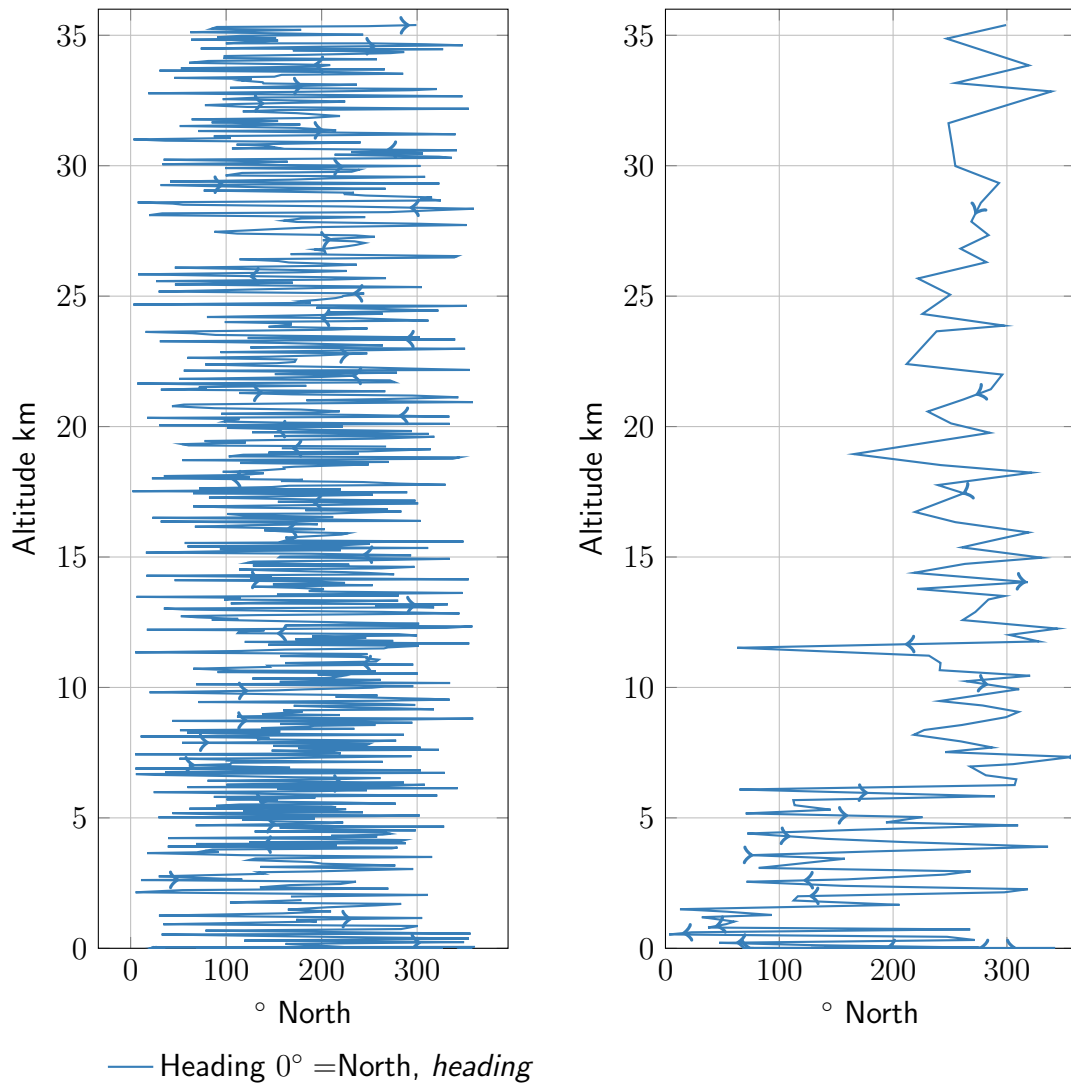


Figure 25: Heading of Titan 1’s payload box during ascent and descent. Values derived from earth acceleration readings and earth magnetic field.

After the balloon burst the payload box starts spinning violently with an angular velocity larger than 250° s^{-1} at which the sensor sensitivity limit was set. From the images an angular velocity in the order of 360° s^{-1} seems reasonable. Only once the vertical velocity reduced (see Fig. 7) the payload box spin reduces and stabilizes shortly before touchdown. This is also confirmed when analysing the images.

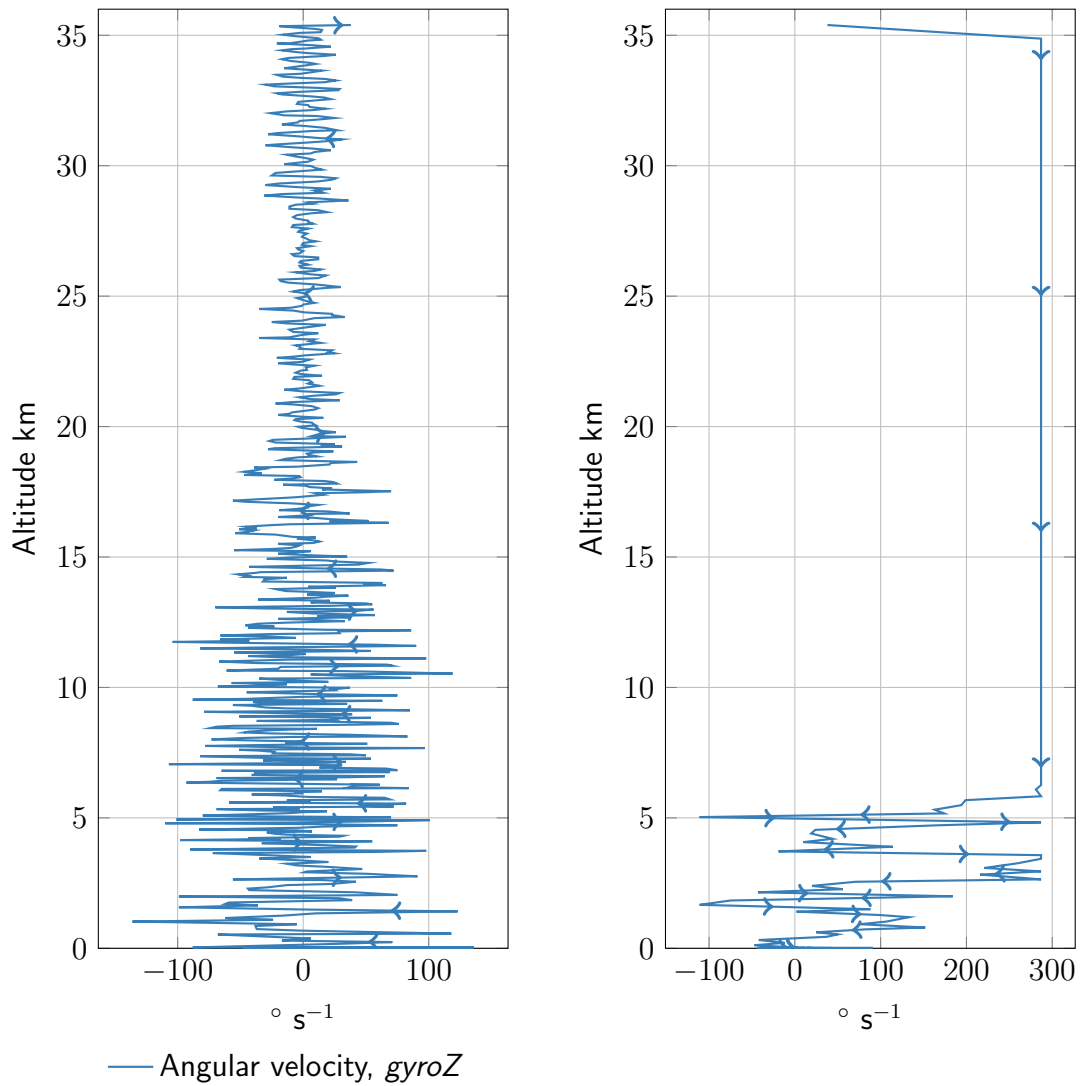


Figure 26: Something gyroZ

Figure 27: Spin around vertical axis of Titan 1’s payload box during ascent and descent. Values derived from gyroscopic sensors.

It is hypothesized that this strong spin around the vertical payload box axis is due to aerodynamic forces created by the not fully deployed parachute and the balloon remains. As once the parachute deploys and reducing the vertical velocity the payload box spins reduces drastically and the payload box gets in a more horizontal position, see roll in Fig. 23 and pitch in Fig. 24.

9 Conclusion

In general it can be concluded that the mission went very well, especially as it was the first mission. The most critical components, flight computer, transmission, balloon and parachute, worked nominal throughout the flight. Equipping Titan 1 with a variety of sensors allowed to evaluate the performance of these sensors under the extrema conditions in high altitude and gain confidence in the individual system components. Further, a lot could be learned of how the components work together in a system exposed to high altitude.

However improvements are necessary for following missions.

- Filling the camera housing with Dust-Off (1,1-Difluoroethane) could not prevent fogging. Thus next time the camera will not be placed inside a closed housing.
- Less of an issue, but an important point is how to fill the balloon correctly while exposed to wind. The prediction should be done with a larger coefficient of variation.
- Sensor operation has to be checked even more, especially if the software drivers are working correctly and in the full operation range.
- The descent time should be estimated not based on the target touchdown velocity.

Some targets for following missions could be:

- Reduce payload weight as much as possible smaller 50 g.
- Go as close to 45 000 m as possible.
- Make a floater and try to get as fare as possible for as long as possible.
- Install a repeater to allow communication via a HAB.
- And many more. . .

A Diagrams of Raw Logged Data

A.1 FLIGHT COMPUTER DATA

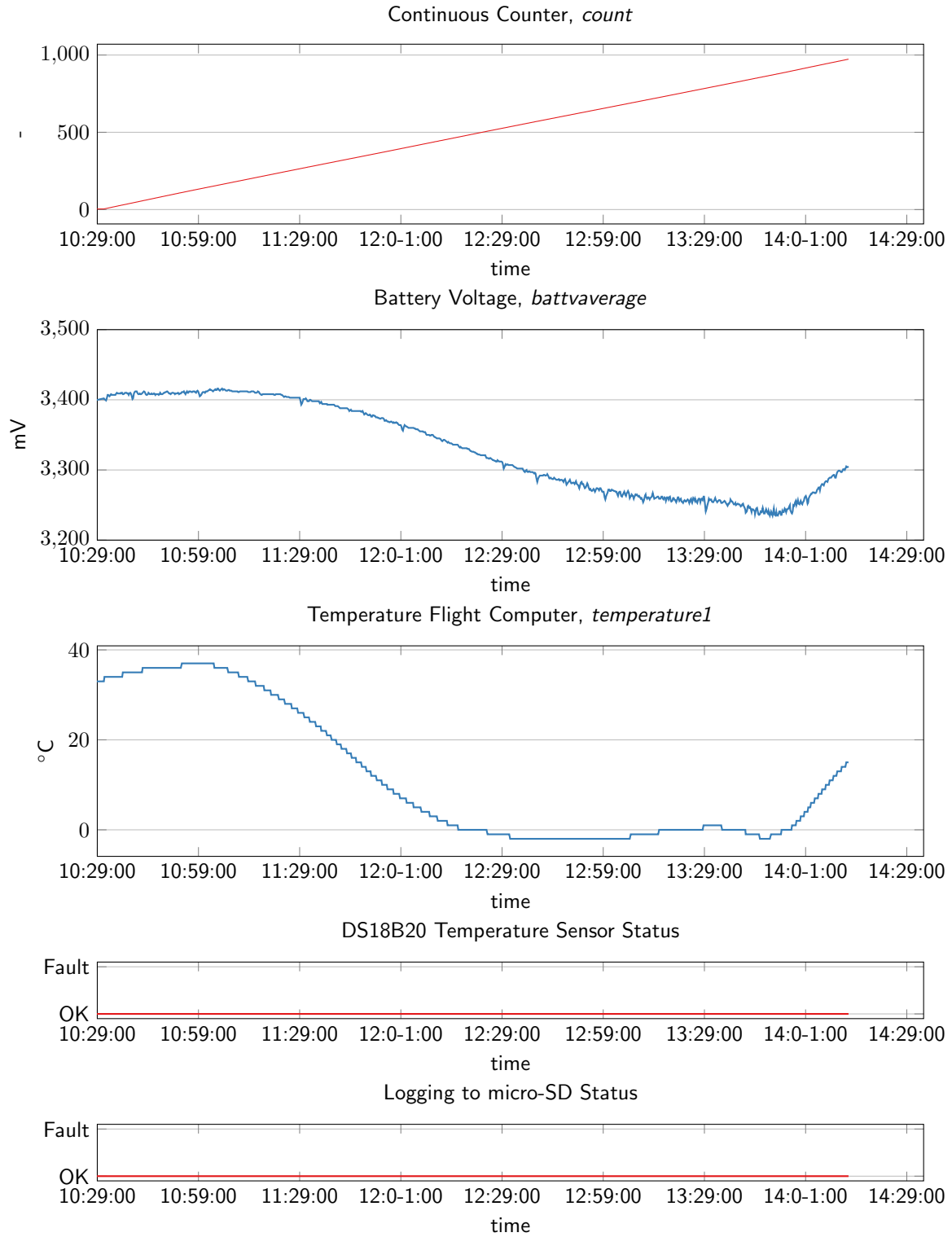


Figure 28: Raw logged data regarding flight computer. Last two plots flight computer temperature sensor status and logging status.

A.2 GPS LOCATION

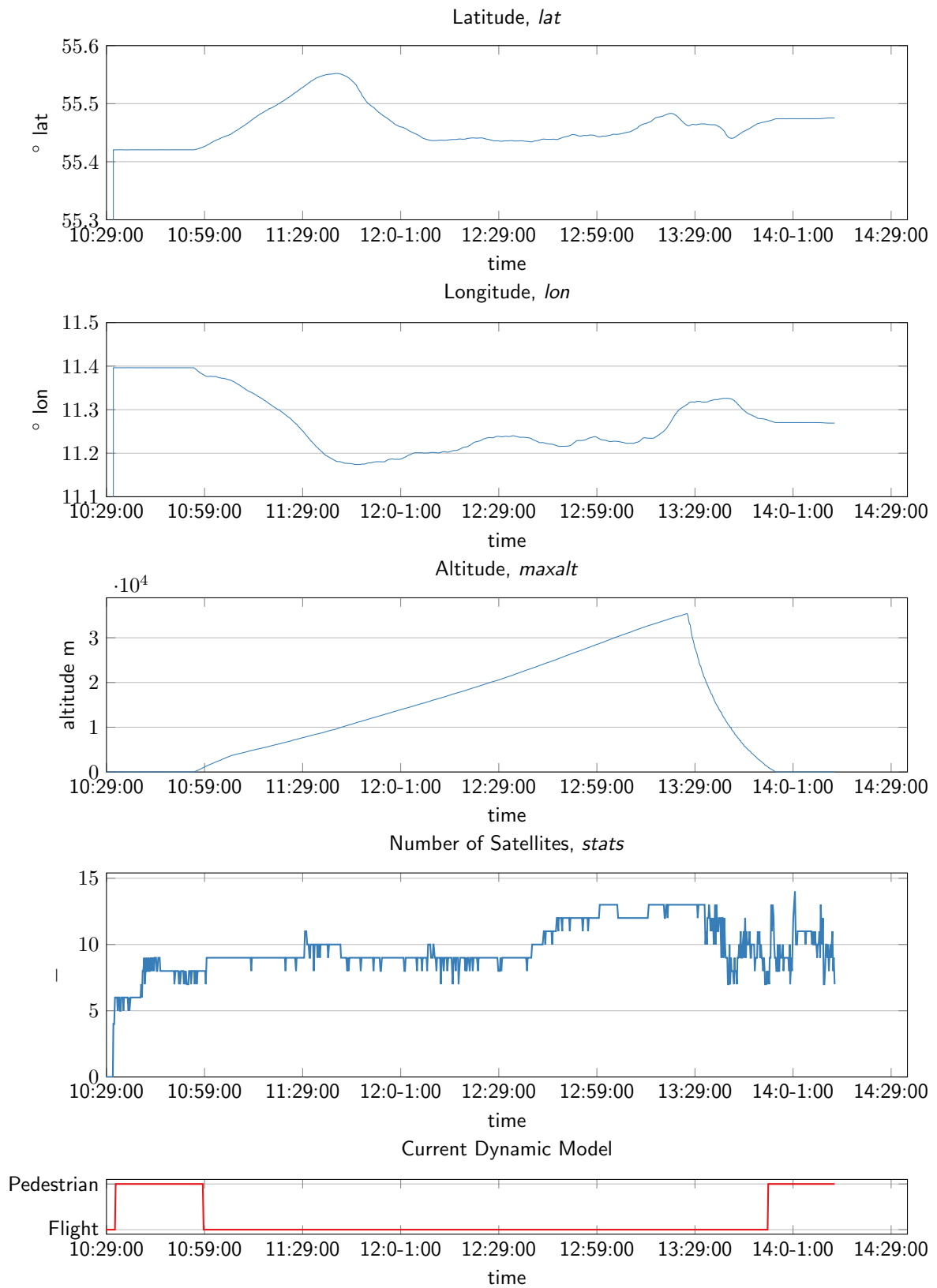


Figure 29: GPS logged location and number of satellites. Last plot GPS dynamic model.

A.3 CHECK STATUS GPS

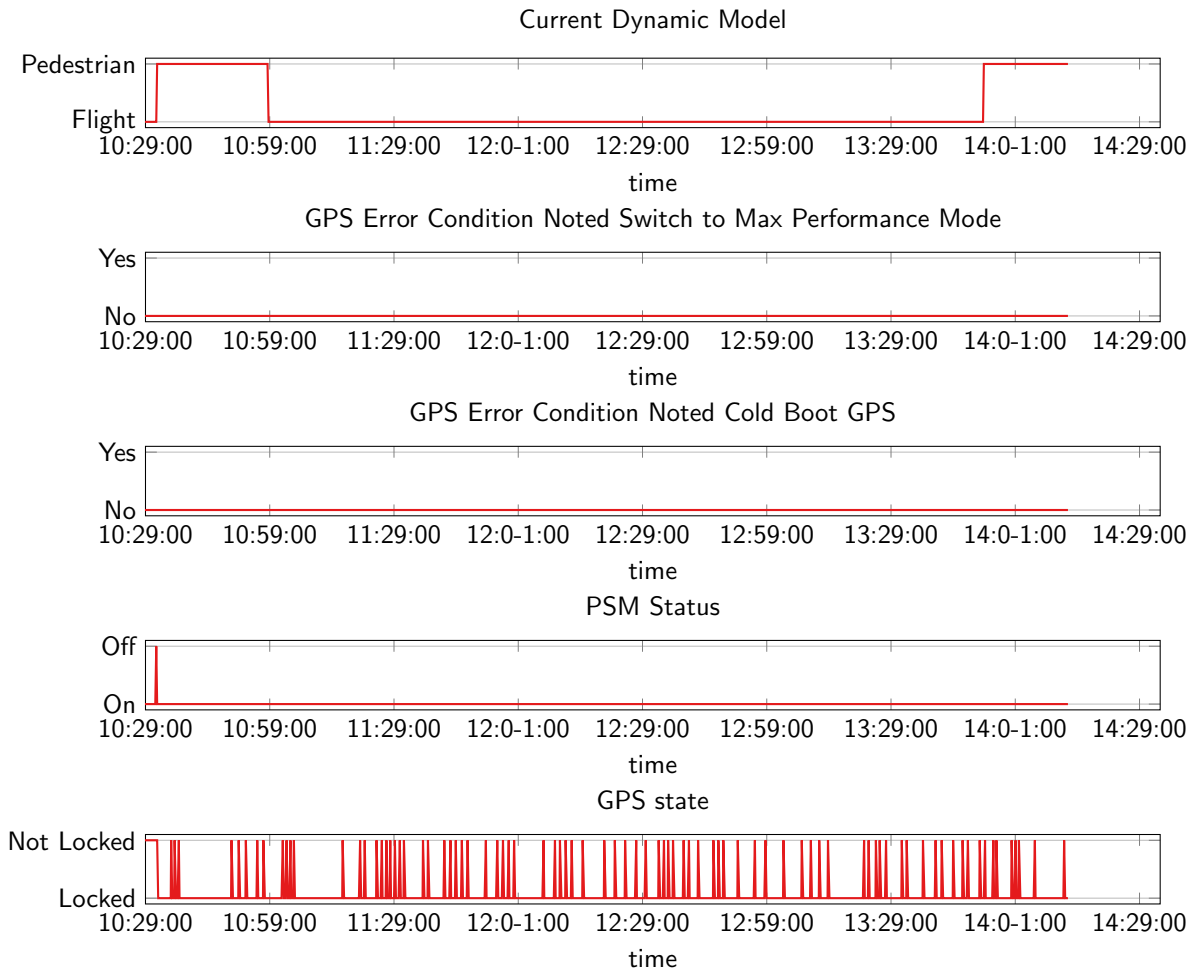


Figure 30: Raw logged data regarding various GPS states.

A.4 LUMINOSITY, TEMPERATURE AND RELATIVE HUMIDITY SENSOR

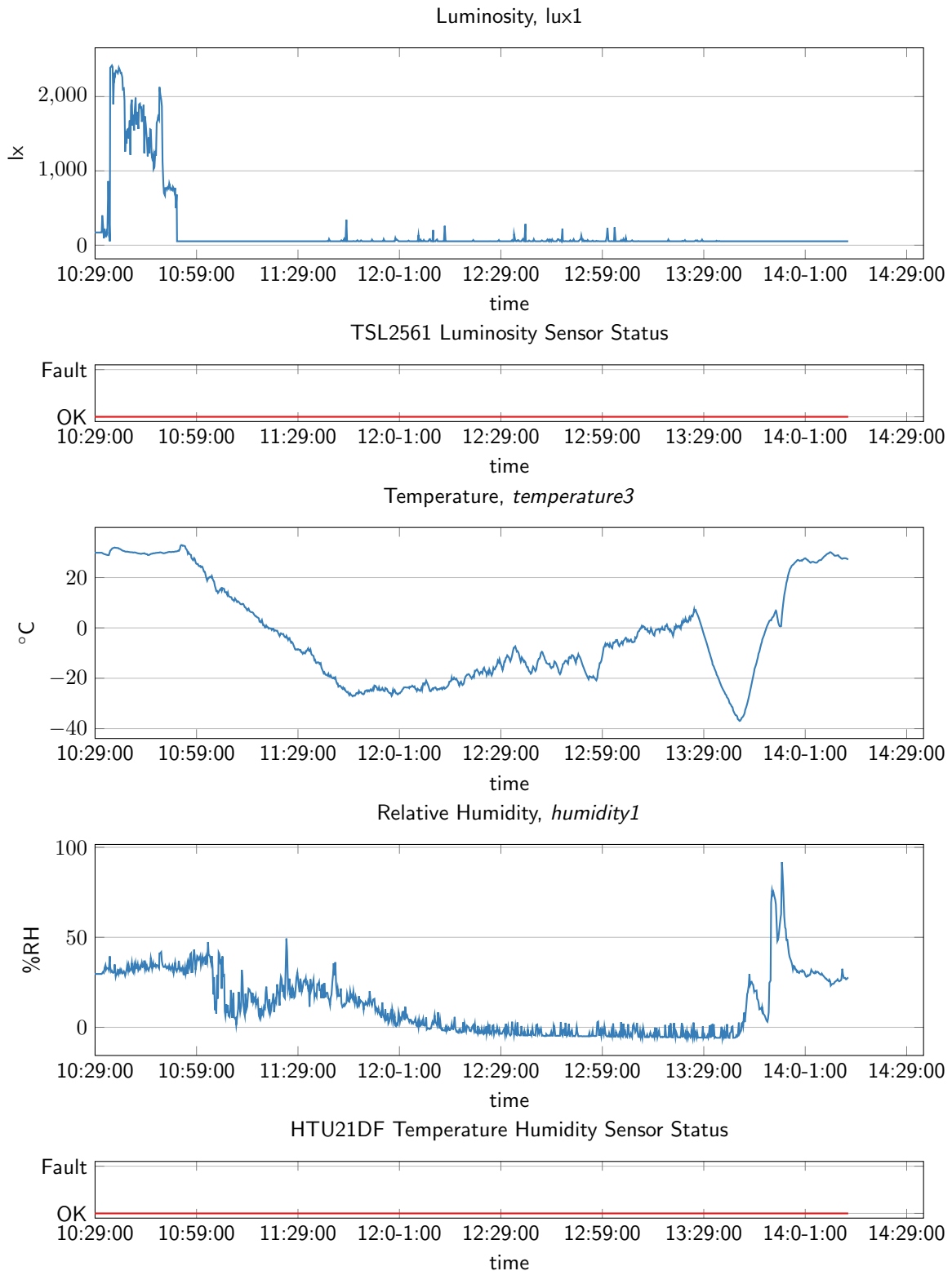


Figure 31: Raw logged data of luminosity, temperature and relative humidity sensors mounted on the outside of the payload box. Second and last plot according sensor status.

A.5 EXTERNAL PRESSURE SENSORS READINGS

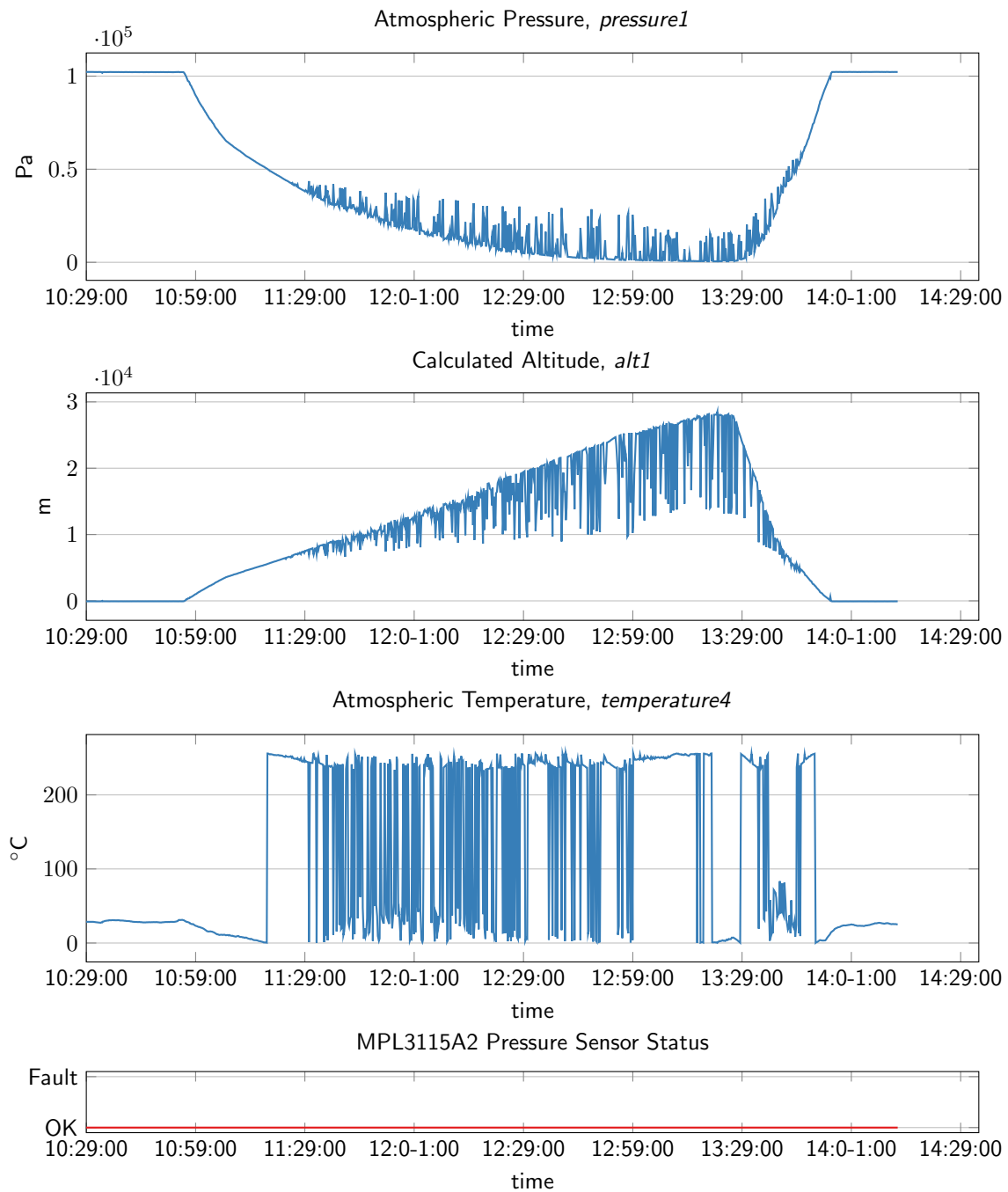


Figure 32: Raw logged data of MPL3115A2 pressure sensor mounted on the outside of the payload box. Last plot sensor status.

A.6 PRECISION TEMPERATURE SENSOR

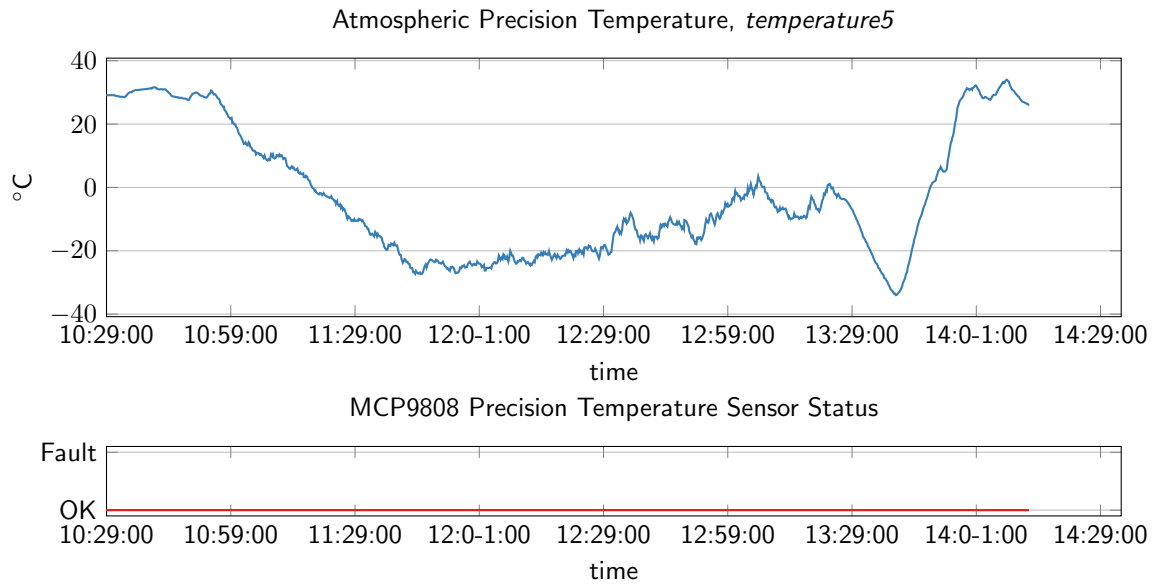


Figure 33: Raw logged data from precision temperature sensor. Last plot sensor status.

A.7 INTERNAL PRESSURE SENSOR READINGS

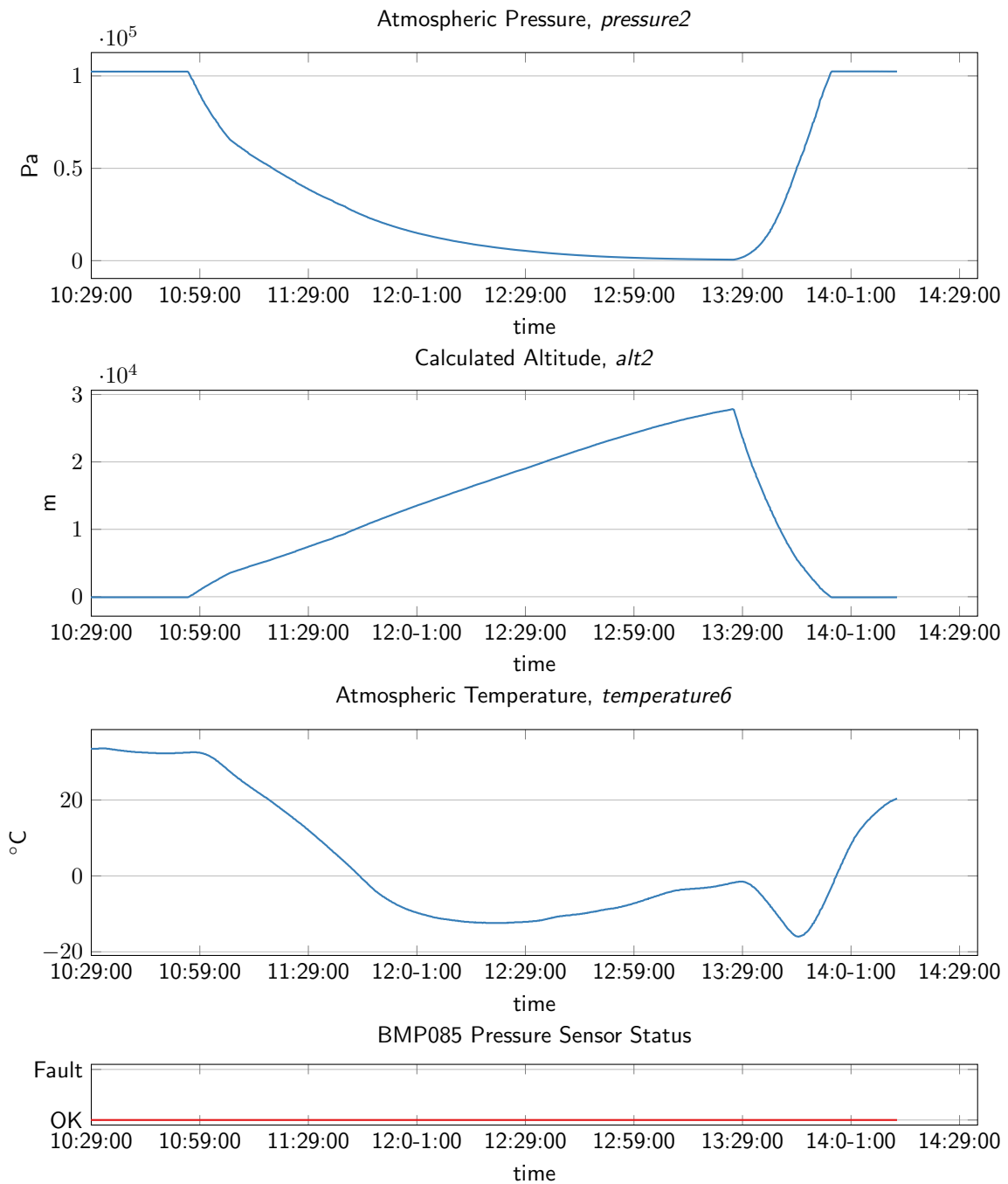


Figure 34: Raw logged data of BST-BMP180 pressure sensor mounted on the inside of the payload box. Last plot sensor status.

A.8 GYROSCOPE SENSOR READINGS

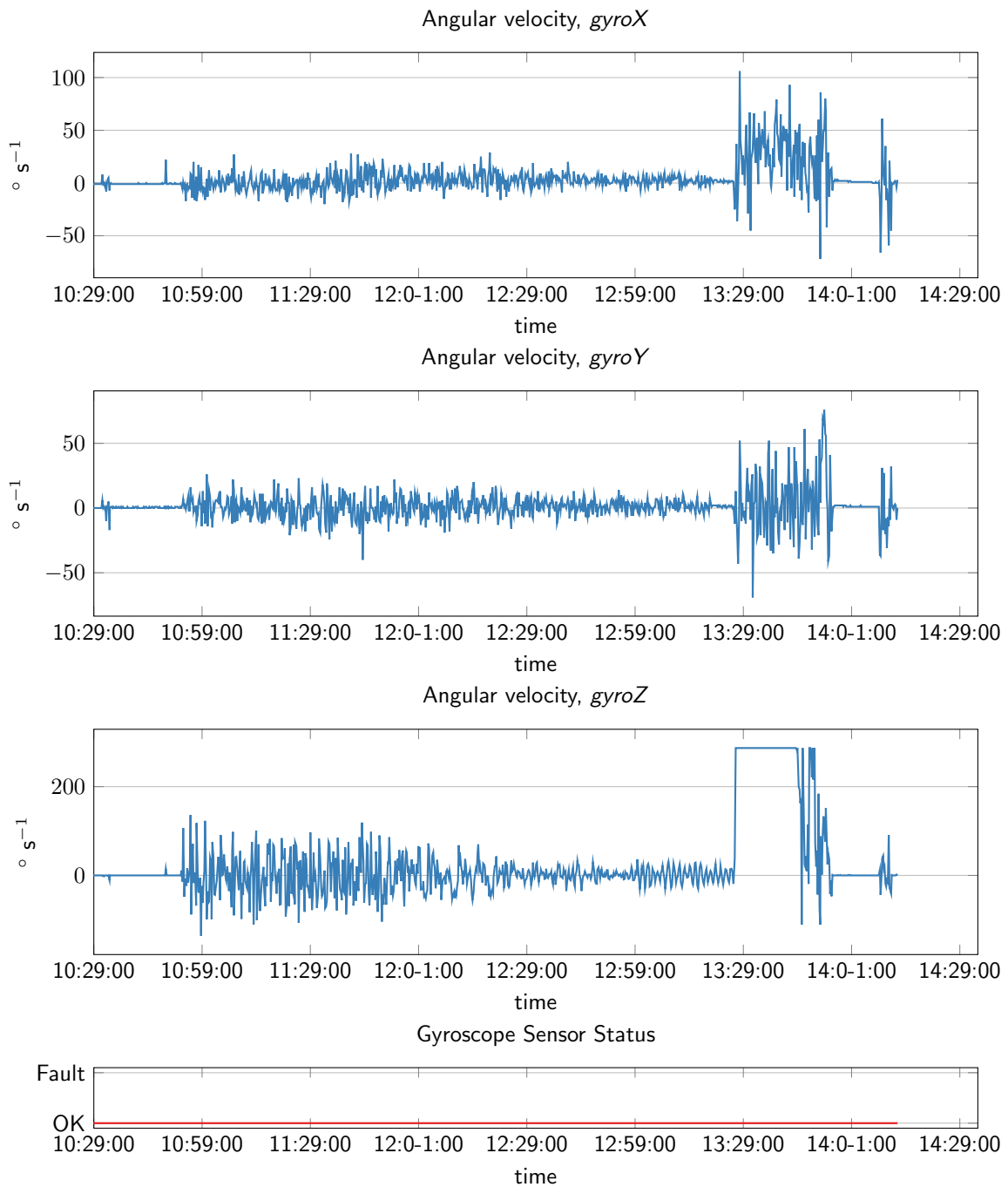


Figure 35: Raw logged data of gyroscope sensor. Last plot sensor status.

A.9 ACCELEROMETER SENSOR READINGS

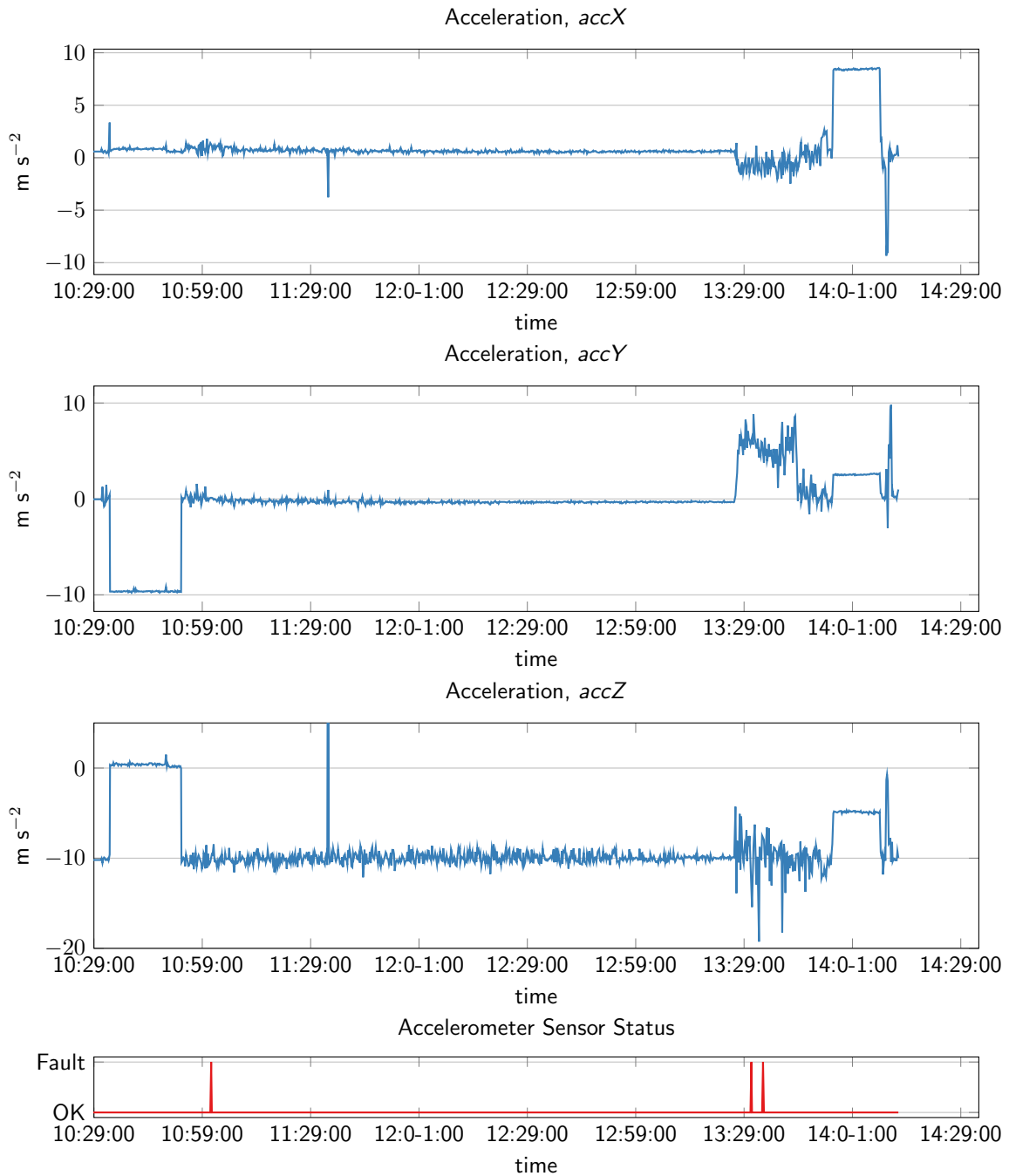


Figure 36: Raw logged data of accelerometer sensor. Last plot sensor status.

A.10 MAGNETOMETER SENSOR READINGS

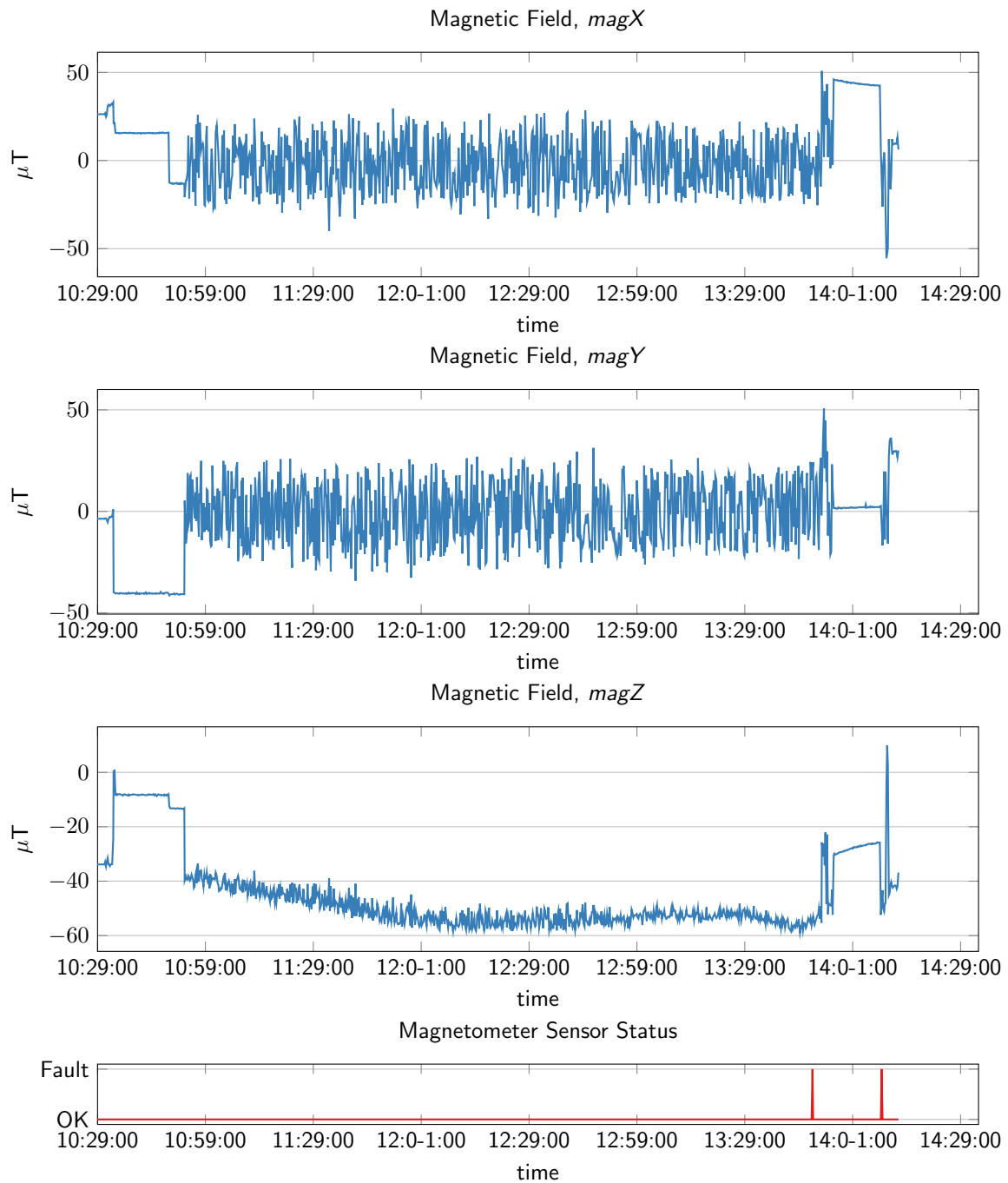


Figure 37: Raw logged values from magnetometer sensor. Last plot sensor status.

A.11 ROLL, PITCH AND HEADING

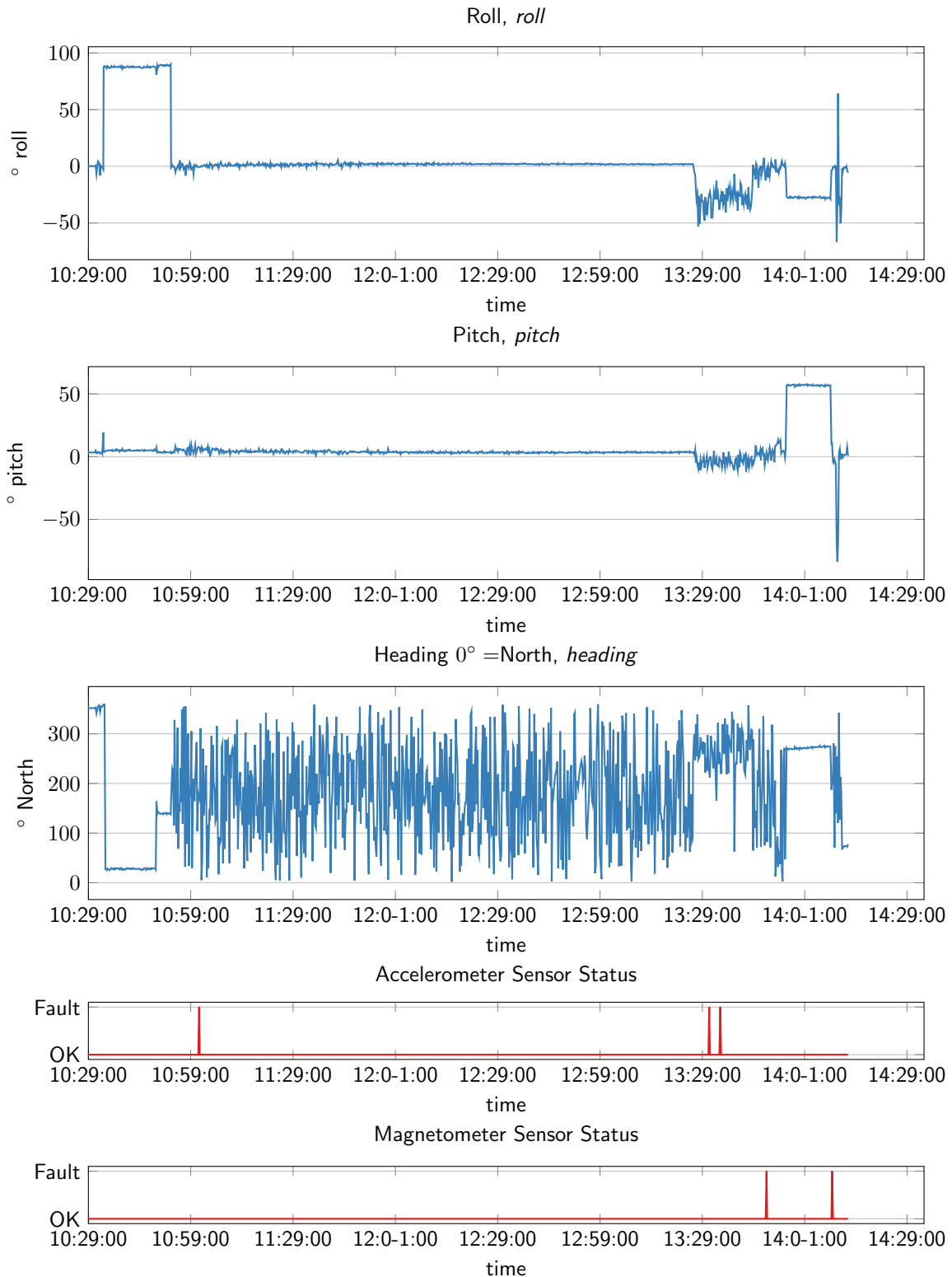


Figure 38: Raw calculated and logged data for roll, pitch and heading. Last two plots sensor status of involved sensors.